

MACHINE FAULT DIAGNOSIS USING A MODIFIED TRANSFERABLE CNN

By

Sanjana Khan Shammi
19166014

A thesis submitted to the Department of Computer Science and Engineering in partial
fulfillment of the requirements for the degree of
Master of Science in Computer Science and Engineering

Computer Science and Engineering
BRAC University
July 2023

© 2023. Sanjana Khan Shammi
All rights reserved.

Declaration

It is hereby declared that

1. The thesis submitted is my/our own original work while completing degree at BRAC University.
2. The thesis does not contain material previously published or written by a third party, except where this is appropriately cited through full and accurate referencing.
3. The thesis does not contain material which has been accepted, or submitted, for any other degree or diploma at a university or other institution.
4. I/We have acknowledged all main sources of help.

Student's Full Name & Signature:

**Sanjana Khan Shammi
19166014**

Approval

The thesis/project titled “MACHINE FAULT DIAGNOSIS USING A MODIFIED TRANSFERABLE CNN” submitted by

1. Sanjana Khan Shammi (19166014)

of Summer, 2023 has been accepted as satisfactory in partial fulfillment of the requirement for the degree of MSc in Computer Science on August 6, 2023.

Examining Committee:

Supervisor and Program Coordinator:
(Member)

Dr Amitabha Chakraborty
Professor, Computer Science and Engineering
BRAC University

External Expert Examiner:
(Member)

Dr. Mohammad Zahidur Rahman
Professor, Computer Science and Engineering
Jahangirnagar University

Internal Expert Examiner:
(Member)

Md. Golam Rabiul Alam, Ph.D
Professor, Computer Science and Engineering
BRAC University

Internal Expert Examiner:
(Member)

Dr. Muhammad Iqbal Hossain
Associate Professor, Computer Science and Engineering
BRAC University

Departmental Head:
(Chair)

Sadia Hamid Kazi, Ph.D
Chairperson and Associate Professor
Department of Computer Science and Engineering
BRAC University

Abstract/ Executive Summary

Detecting prior bearing faults is an essential task of machine health monitoring because bearings are the crucial parts of rotating machines. The performance of traditional intelligent fault diagnosis methods depends on feature extraction of fault signals, which requires signal processing techniques, expert knowledge, and human labor. Deep learning algorithms have recently been applied for industrial machine health monitoring with their advanced features. With the capacity to automatically learn complex features of input data, deep learning architectures have great potential to overcome the drawbacks of traditional intelligent fault diagnosis. This paper proposes a rolling bearing fault diagnosis method based on Convolutional Neural Network and Leaky ReLU to solve the above problems. Firstly, the Continuous Wavelet Transform converts one-dimensional original vibration signals into two-dimensional time-frequency images. Secondly, the obtained time-frequency images are used to train the constructed model. Finally, the diagnosis of the fault location and severity is completed. The method is verified on the MFPT, MIMII data set, and vehicle engine. The results demonstrate that the suggested approach achieves higher diagnostic accuracy which is 95.49% on average and 2% greater than other advanced techniques. We have also incorporated XAI in the input images to make the network more transparent.

Keywords: Transfer Learning, CNN, SqueezeNet, ResNet18, Leaky ReLU, XAI

Dedication (Optional)

This study is wholeheartedly dedicated to our beloved parents, who have been our source of inspiration and gave us strength when we thought of giving up, who continually provide their moral, spiritual, emotional, and financial support.

To my beloved spouse who shared his words of advice and encouragement to finish this study. And lastly, we dedicated this book to the Almighty God, thank you for the guidance, strength, power of mind, protection, and skills and for giving us a healthy life.

Table of Contents

Declaration	ii
Approval.....	iii
Abstract/ Executive Summary	iv
Dedication (Optional).....	v
Table of Contents	vi
List of Tables.....	viii
List of Figures.....	ix
List of Acronyms	xi
Glossary	xii
Chapter 1 Introduction	13
1.1 Overview	14
1.2 Problem Statement.....	15
1.3 Research Objective	17
1.4 Methodology	18
1.5 Thesis Outline.....	19
Chapter 2 Literature Review	20
2.1 CWT for 1D Signal Processing	20
2.2 Convolutional Neural Network	21
2.3 Activation Funtions	26
2.4 State of Art	27

Chapter 3 The Proposed CNN-LR Model.....	30
3.1 Design of CNN-LR Model.....	30
3.2 Proposed Method of Industrial Machine Fault Diagnosis	33
Chapter 4 Experimental Setup	37
4.1 MFPT Dataset.....	37
4.1.1 Data Description.....	37
4.1.2 Data Processing	38
4.1.3 Results of the Experiment.....	40
4.2 MIMII Dataset	43
4.2.1 Data Description.....	43
4.2.2 Data Processing	45
4.2.3 Results of the Experiment.....	47
4.3 Vehicle Engine Dataset	50
4.3.1 Data Description.....	50
4.3.2 Data Processing	52
4.3.3 Results of the Experiment.....	54
4.4 Explainable Artificial Intelligence (XAI)	56
4.5 Result Analysis	58
Chapter 5 Conclusion and Future Work.....	60
References.....	61
Appendix A.....	1

List of Tables

Table 1: State of Art	28
Table 2: Structure and parameters of standard SqueezeNet	31
Table 3: Structure and parameters of standard ResNet-18	32
Table 4: The sample description of MFPT dataset	38
Table 5: Accuracy Comparison between Standard SqueezeNet, Standard ResNet-18, proposed CNN-LR model and proposed CNN-PR model	41
Table 6: MIMII dataset content details	44
Table 7: Detail data of selected MIMII dataset file	45
Table 8: Accuracy Comparison between Standard SqueezeNet, Standard ResNet-18 and proposed CNN-LR model of MIMII dataset	48
Table 9: Vehicle details from which sample data collected	51
Table 10: The sample description of Vehicle Engine dataset	52
Table 11: Accuracy Comparison between Standard SqueezeNet, Standard ResNet-18 and proposed CNN-LR model of Vehicle Engine dataset	55
Table 12: Average accuracy and average training time of four CNN models	59

List of Figures

Figure 1: Top Level Overview	18
Figure 2: Conversion process from 1D time-domain signal to 2D time-frequency image	20
Figure 3: Hidden Layers of Convolutional Neural Network.....	23
Figure 4: Network architecture of SqueezeNet (a) and ResNet-18 (b).....	25
Figure 5: Network architecture of Standard ResNet-18 with ReLU activation function (a) and Modified ResNet-18 with Leaky ReLU Function (b)	31
Figure 6: The flowchart of experiment	36
Figure 7: Time-frequency images of three health conditions on MFPT dataset: (a) Baseline; (b) Outer; (c) Inner.	40
Figure 8: Training Progress of CNN_LR model of MFPT Dataset.....	41
Figure 9: Confusion matrix of MFPT dataset for (a) Standard SqueezeNet; (b) Standard ResNet-18 and (c)CNN-LR Model (d)CNN-PR Model	42
Figure 10: Time-frequency images of three health conditions on MIMII dataset: (a) Abnormal pump dataset (b) Normal pump dataset.....	46
Figure 11: Training Progress of CNN_LR model of MIMII Dataset	47
Figure 12 Confusion matrix of MIMII dataset four types of machine identification for (a) Standard SqueezeNet; (b) Standard ResNet-18 and (c) Proposed CNN-LR Model.....	49
Figure 13: Confusion matrix of MIMII dataset for (a) Standard SqueezeNet; (b) Standard ResNet-18; (c) Proposed CNN-LR Model and (d) Proposed CNN-PR Model.....	50
Figure 14: Images of Transport Vehicle of Saintmartin Travels; (a) Normal/new sleeper coach, (b) Engine of normal/new sleeper coach, (c) Faulty/Old bus, (d) Engine of faulty/old bus, (e) taking sample of engine sound and (f) Photo with Director of Saintmartin Travels	52
Figure 15: Time-frequency images of two classes on Vehicle Engine dataset: (a) Abnormal vehicle engine dataset (b) Normal vehicle engine dataset	53

Figure 16: Training Progress of CNN_LR model of Vehicle Engine Dataset 54

Figure 17: Confusion matrix of Vehicle Engine dataset for (a) Standard SqueezeNet; (b) Standard ResNet-18; (c) Proposed CNN-LR Model and (d) Proposed CNN-PR Model 56

Figure 18: Comparison of XAI methods on MFPT, MIMII and Vehicle Engine datasets 57

Figure 19: Classification accuracy and comparison of four different CNN models on three different datasets 58

List of Acronyms

CNN	Convolutional Neural Network
XAI	Explainable Artificial Intelligence
TL	Transfer Learning
ReLU	Rectified Linear Unit
LR	Leaky ReLU
CWT	Continuous Wavelet Transform
MIMII	Malfunctioning Industrial Machine Investigation and Inspection
MFPT	Machinery Failure Prevention Technology
PR	Parametric ReLU
LIME	Local Interpretable Model-agnostic Explanations
Grad-CAM	Gradient-weighted Class Activation Mapping
IFD	Intelligent Fast Detection

Glossary

- Thesis: An extended research paper that is part of the final exam process for a graduate degree. The document may also be classified as a project or collection of extended essays.
- Glossary: An alphabetical list of key terms

Chapter 1

Introduction

In today's industrial landscape, the smooth operation of machinery is crucial for maintaining productivity and minimizing downtime. However, faults and malfunctions are inevitable, potentially leading to costly disruptions and safety hazards. In the recent report by Senseye, the AI-powered machine health management company, has researched that Large industrial facilities lose more than a day's worth of production each month and hundreds of millions of dollars a year to machine failures. The report "The True Cost Of Downtime" shows that large plants lose an average of 323 production hours per year, costing \$172 million annually due to lost revenue, financial penalties, idle staff time, and restarting lines. Cumulatively, manufacturing and industrial firms on the Fortune Global 500 list lose an estimated 3.3 million hours per year to unplanned downtime, which costs them \$864 billion annually, equivalent to 8% of their revenues [37].

Industrial downtime is a costly problem that affects all sectors. Alexander Hill, chief global strategist at Senseye, warns that when machinery breaks down, it can cost manufacturers over \$100,000 per hour in lost revenue. On average, automotive plants lost 29 production hours a month due to unplanned downtime, costing \$1.3 million per hour. This led to approximately \$557 billion and 414,800 lost annual hours for automakers and suppliers. Senseye's study revealed that 72% of large manufacturers have made predictive maintenance a strategic objective and 20% have established in-house teams to lead these initiatives [37].

In Bangladesh, it is evident from recent news and articles that businesses are losing significant revenue due to decreased production rates caused by faults in their manufacturing machines. Therefore, efficient fault diagnosis techniques are essential to identify and address these issues

promptly. With recent advancements in deep learning and artificial intelligence, Convolutional Neural Networks (CNNs) have emerged as powerful tools for automated fault diagnosis [1]. This thesis focuses on developing an advanced and modified Transferable CNN for fault diagnosis of industrial machinery, incorporating explainable Artificial Intelligence (XAI) techniques [2] [3].

1.1 Overview

This thesis aims to develop advanced CNN model for fault diagnosis of industrial machines. The primary objective is to develop a comprehensive network architecture that combines advanced data processing techniques and machine learning algorithms to enable efficient fault detection and classification.

This research begins with data collection where we have worked with three different datasets, one is MFPT, second one is MIMII and another one real engine dataset from a transportation company. For the MFPT dataset, we have collected the data from the open internet which is for rolling bearing faulty data [9]. For MIMII dataset, we have collected normal and faulty data of industrial fan from open internet [23]. Lastly, for real dataset, we have collected faulty engine sound and normal engine sound from a transportation bus from a local company of Bangladesh [24].

Following this, all the inputs are processed with advanced signal processing tool Continuous Wavelet Transform. Noise reduction of the vibration signal by CWT can express the fault features of the vibration signal more accurately and comprehensively. Hence, CWT is used to analyze the vibration signal in the time-frequency domain, draw the vibration signal time-frequency diagram, and save it to the designated folder [27].

After signal processing, we have deployed two existing architectures of CNN and our proposed architecture where we have changed the activation function in the hidden layers. We have trained the three mentioned datasets with all three models and the final result is compared in the bar chart. We have implemented XAI algorithms to identify fault characteristics, allowing CNN models to

provide results. When a model is considered a black box, the user receiving the diagnosis does not know how the model reached the final conclusion. This lack of transparency compromises the reliability of the diagnosis, making it less likely to be used. Studies have been developed to explain why a model's final classification was obtained. The Gradient-weighted Class Activation Mapping (Grad-CAM) is currently the state-of-the-art approach in post-hoc methods that provide visual explanation. It is useful to identify faults in IFD through a heatmap that highlights the most relevant frequencies for classification, overlaid on the input signal, as faults are typically identified through visual analysis of the signal in the frequency domain.

In conclusion, this thesis aims to contribute to the field of fault diagnosis for industrial machines by developing a comprehensive and effective framework by working with the hidden layers of CNN network. By addressing the limitations of existing techniques and leveraging advanced data analysis and machine learning algorithms, this research seeks to enhance fault detection capabilities, reduce maintenance costs, and improve overall system reliability [31].

1.2 Problem Statement

Fault diagnosis of industrial machinery is a critical task in ensuring the smooth operation and productivity of manufacturing systems. Traditional approaches to fault diagnosis often rely on manual inspection or rule-based methods, which can be time-consuming, labor-intensive, and prone to human errors. There is a need for an automated and efficient system that can accurately detect and diagnose faults in industrial machinery [28].

Convolutional Neural Networks (CNNs) have shown great potential in various computer vision tasks, including image classification and object detection. However, the application of CNNs to fault diagnosis of industrial machinery poses specific challenges. These challenges include the complex nature of industrial machine data, such as vibration signals, acoustic signals, or thermal images, which require specialized preprocessing techniques to extract relevant features [29].

The traditional approach to fault diagnosis of industrial machinery through CNN involves several steps. Firstly, a large dataset of labeled samples comprising both normal and faulty machine conditions is required for training the CNN model. The dataset needs to capture a wide range of fault types and severities to ensure the model's robustness. Secondly, preprocessing techniques are employed to extract meaningful features from the raw data. This may involve techniques such as time-frequency analysis, wavelet transforms, or spectrogram analysis to convert the time-domain signals into a format suitable for input to the CNN. Next, the CNN model is designed and trained using the labeled dataset. This involves selecting an appropriate architecture, determining hyperparameters, and training the model on the labeled data. The training process typically involves optimizing a loss function, such as categorical cross-entropy, through techniques like backpropagation and gradient descent. Once the CNN model is trained, it can be used for fault diagnosis by inputting new, unlabeled data. The model analyzes the input data and predicts the presence of faults and, in some cases, provides insights into the specific fault type or severity. Despite the promising capabilities of CNNs, the traditional approach of fault diagnosis through CNN still faces challenges. These include the need for large and diverse labeled datasets, the selection of appropriate preprocessing techniques, and the interpretability of the CNN model's predictions [30].

Therefore, the aim of this paper is to compare and analysis the traditional approach of fault diagnosis of industrial machinery through CNN, including its challenges and potential solutions, to contribute to the advancement of automated fault diagnosis systems for industrial applications. In this paper, the architecture of CNN networks is modified to solve the back propagation problem of traditional approach.

1.3 Research Objective

The objective of this research paper is to compare and analysis the effectiveness of the traditional approach of fault diagnosis of industrial machinery through Convolutional Neural Networks (CNN) and to propose new approach which provides better accuracy than existing approaches.

The study aims to accomplish the following objectives:

Firstly, the research will evaluate the accuracy and efficiency of CNN models in detecting and diagnosing faults in industrial machinery. This objective includes analyzing the impact of different CNN architectures on the diagnostic performance.

Secondly, the study will examine various preprocessing techniques, such as time-frequency analysis, wavelet transforms, and spectrogram analysis, to extract relevant features from raw industrial machine data. The objective is to evaluate the effectiveness of these techniques in enhancing fault detection accuracy and reducing false positives/negatives by working with the hidden layers.

In this research, we have worked with three different datasets. First one is MFPT dataset [9] where we have taken the data for rolling bearing machines. Second dataset is MIMII dataset [23] where the data of industrial fan is collected for the experiment. For the third and customized dataset, we have collected the data from vehicle engine of Saintmartin Travels [24], a transportation company of Bangladesh. This objective aims to assess the impact of dataset size and diversity on the CNN model's performance and generalization capabilities.

The study will explore and integrate Explainable Artificial Intelligence (XAI) techniques into the CNN model to improve interpretability and provide explanations for the model's decision-making process. This objective includes investigating methods such as saliency maps, attention mechanisms, or feature visualization to highlight the regions or features influencing the model's fault diagnosis predictions [3].

By addressing these research objectives, the paper aims to contribute to the understanding and advancement of fault diagnosis techniques using CNNs for industrial machinery, facilitating the development of more accurate and automated systems for real-world applications.

1.4 Methodology

The methodology followed in this paper is shown in Fig 1. In this research, a network architecture based on CNN and Leaky ReLU is established for rolling bearing fault diagnosis, which we call CNN-LR model. This chapter mainly includes the structure and design of CNN-LR model and industrial machine fault diagnosis based on the proposed model.

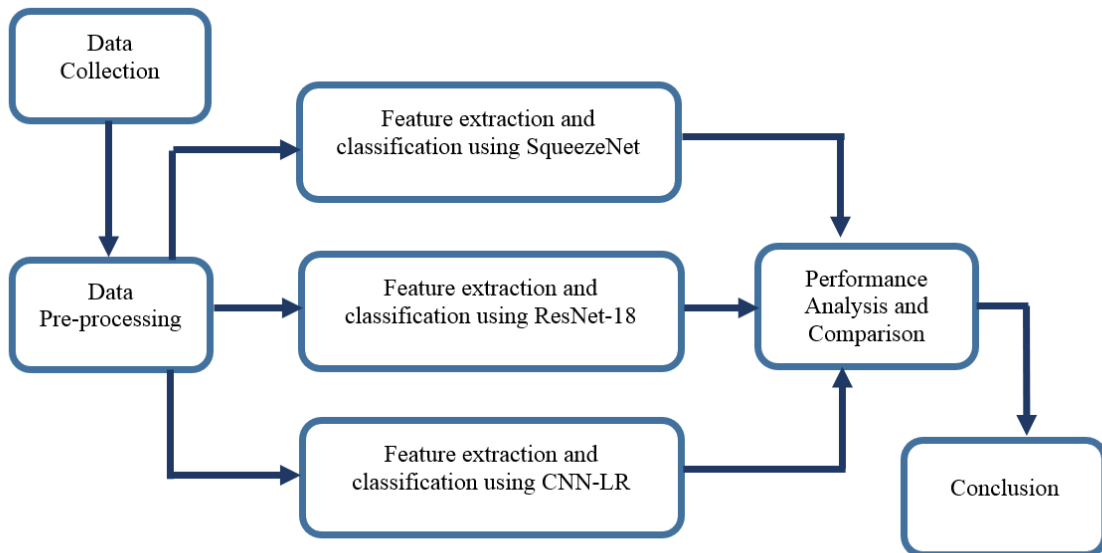


Figure 1: Top Level Overview

First, faulty and normal audio vibration were collected from three datasets. In this research, we have implemented the whole experiment into three kind of datasets. All the details of three datasets are mentioned in the subchapter 3.1. These datasets were stored as MATLAB files as one-dimensional format. They were then pre-processed for 2-D CNN input, each sample was created from 12,496 data points; for the 2-D CNN input, a two-dimensional image representation

of 227×227 pixels was created for SqueezeNet, 224×224 pixels was created for ResNet18 and proposed ResNet18 model. We then used each model to perform feature extraction and classification. Finally, we performed a performance analysis and drew conclusions.

1.5 Thesis Outline

This paper is organized with below thesis outline:

Chapter 2 Literature Review

This chapter is dedicated to the theory of CWT, CNN and Leaky ReLU following with the state of the art of related work.

Chapter 3 The Proposed CNN-LR Model

The design of CNN-LR model is explained in this chapter with our proposed method for Industrial Machine Fault Diagnosis.

Chapter 4 Experimental Setup

In this chapter we have done the experiment with three different dataset: MFPT, MIMII and Real Dataset. All three datasets are explained with description, data pre-processing and result of the experiment. At the end of these chapter, we have also included XAI.

Chapter 5 Conclusion

Finally, the paper has been concluded with the summary of our proposed method that provided better accuracy and also mentioned the future opportunities to improvise our method.

Chapter 2

Literature Review

This paper proposes an intelligent diagnosis method for industrial machinery fault diagnosis. Firstly, we convert the original vibration signals into time-frequency images using CWT. Then, CNN is applied to extract the in-depth features of the time-frequency images. Finally, the ReLU layer is replaced with Leaky ReLU using MATLAB. The following fundamental theories of CWT, CNN, and Leaky ReLU are introduced.

2.1 CWT for 1D Signal Processing

The CWT time-frequency analysis technique efficiently focuses on the signal using scaling and translation operations at various scales. Therefore, CWT can automatically adapt to the requirements of time-frequency signal analysis, clearly describing the change in signal frequency with time. [6]. Here, CWT is used for preliminary feature extraction, converting the original 1-D time-domain signals into 2-D time-frequency images. The conversion process is shown in Fig. 2 [7].

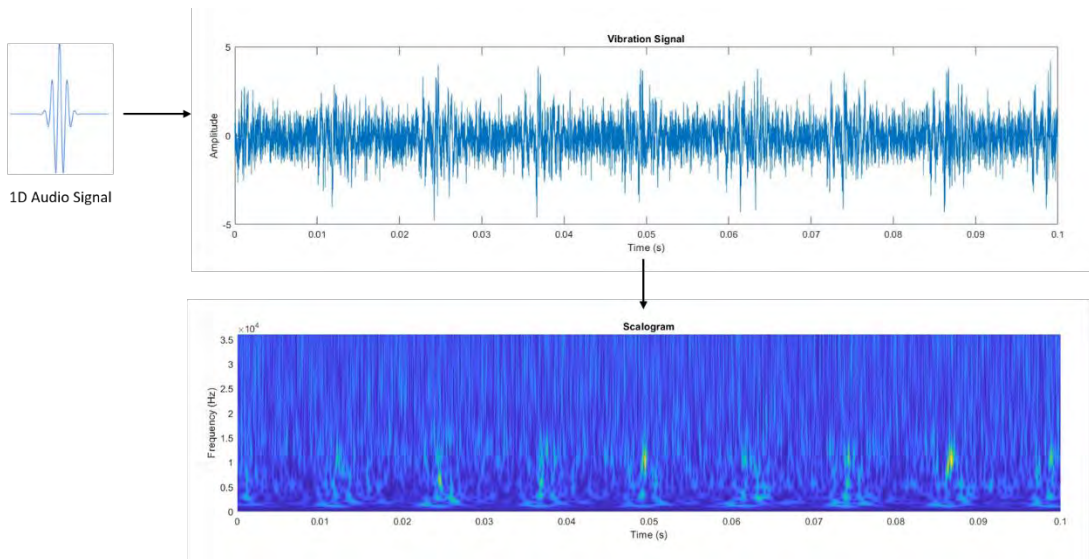


Figure 2: Conversion process from 1D time-domain signal to 2D time-frequency image

CWT is a technique used to extract distinctive signal data that can then be utilized to analyze and manipulate nonlinear signals. Its algorithm is relatively mature, and the basic definition can be expressed as [8]:

$$W_{\varphi}(a, b) = \frac{1}{\sqrt{a}} \int x(t) \varphi^* \left(\frac{t-b}{a} \right) dt, \quad a > 0 \quad (1)$$

In this formula, a is the scale parameter, b is the time or translation parameter, $x(t)$ represents the original one-dimensional data signal, φ represents the wavelet function with scale a and position offset b , and φ^* is the complex conjugate of φ .

2.2 Convolutional Neural Network

Industrial machine fault diagnosis using sound is a technique that involves analyzing the sounds produced by machines in order to detect and diagnose any potential faults or abnormalities. A sound-based fault diagnosis is a valuable tool in industries where machines and equipment play a crucial role, such as manufacturing, automotive, aerospace, and power generation [8]. In rolling element bearings, localized faults can occur in different components, such as the outer race (outer ring), the inner race (inner ring), the cage (which holds the rolling elements in place), or one of the rolling elements (balls or rollers) [9]. These faults can result from various issues, such as wear, pitting, cracks, or improper lubrication. As this is much defined to analyze and detect faults in industrial machinery, sound analysis plays a vital role; many research and techniques have been established to determine the optimum strategy. The research shows that Artificial Neural Network (ANN) has been chiefly used as an algorithm [21]. An ANN has three components for its most popular form: an input layer, a hidden layer, and an output layer. Units in the hidden layer are called hidden units because their values are not observed. Artificial neural networks (ANNs) use algorithms to mimic neurological functions, such as learning from experiences, generalizing from similar situations, and evaluating past poor outcomes [10].

However, it is not easy for many tasks to know what features should be extracted to feed to the AI algorithms. The utilization of deep learning techniques can surpass the shortcomings of current intelligent fault diagnosis techniques by using feature hierarchies that include lower-level features that are composed to form higher-level features. When using deep learning techniques, the system can learn how to map the input to output by automatically learning features at various levels of complexity. This enables the system to grasp complex functions directly from the data. In order to comprehend intricate functions, it is crucial to employ deep architectures that comprise multiple levels of non-linear operations. Deep learning-based methods utilize deep architectures to capture representation information from natural input signals through non-linear transformations. With a small error, they can adaptively approximate complex non-linear functions [11].

Several deep learning methods have already been used for fault diagnosis of rotating machines, such as deep auto-encoder [12], sparse filtering [13], and deep belief network (DBN). DL has achieved better results as compared to traditionally used ML algorithms. Nevertheless, the usability of DL methods for fault diagnosis is yet to be explored. CNN is a popular and more efficient DL approach that has also been applied in the fault classification of rotating machines. The raw vibration signature acquired from the machine is a time-domain signal; the 1D CNN has been applied to monitor the bearing condition [14]. Some researchers have converted signals into images, then applied a 2D CNN to classify the bearing conditions [11].

When using a CNN for fault detection of roller element bearings, the raw or pre-processed sensor data, such as vibration signals or sound recordings, is fed as input to the CNN model. The CNN comprises different layers, such as convolutional, pooling, and fully connected layers, which work together to create hierarchical representations of the input data. The following are definitions of different layers shown in Fig 3 [11].

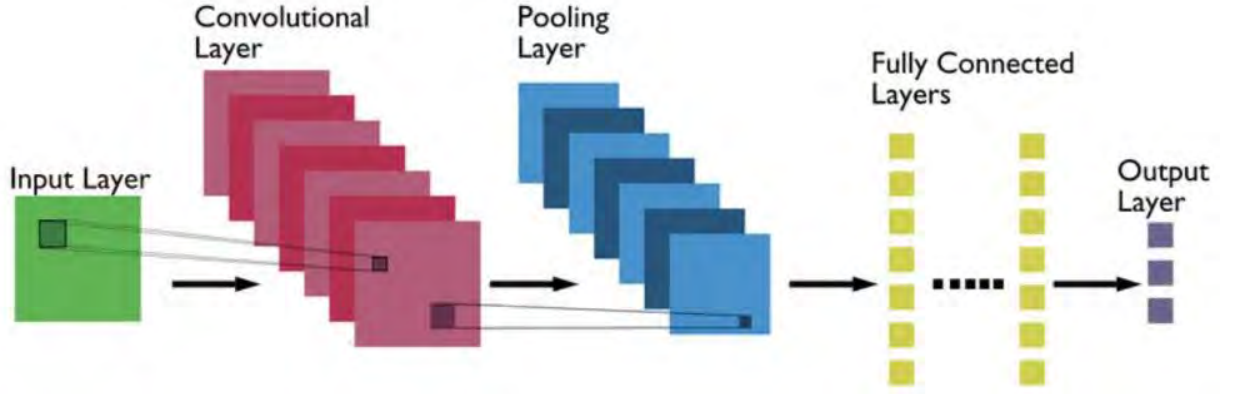


Figure 3: Hidden Layers of Convolutional Neural Network

Convolutional layer: A more advanced feature representation is obtained through convolution operations in the convolution layer. The number of network parameters is decreased, and the complexity of the model is reduced by performing local feature extraction on input data. The convolution formula can be defined as follows:

$$x_j^l = f \left(\sum_{i \in M_j} x_i^{l-1} K_{ij}^l + b_j^l \right) \quad (2)$$

where x_j^l is the output of layer l , x_i^{l-1} represents the output of layer $l - 1$, that is, the input of layer l , M_j is the feature set of layer $l - 1$, K_{ij}^l represents the weight matrix, b_j^l represents the network bias, and $f(\cdot)$ represents the activation function.

Pooling layer: In the pooling layer, the data is reduced in size by taking a specific area's average or maximum value. This helps to simplify the network calculations and keep the essential features, resulting in more efficient feature extraction. The calculation method can be expressed as:

$$x_j^l = f (\beta_j^l \text{down}(x_j^{l-1}) + b_j^l)$$

where $\text{down}(\cdot)$ is the down-sampling function, β represents the weight of the network. (3)

Fully connected layer: After being alternately transferred through convolutional and pooling layers, the image features are input into the fully connected layer. The in-depth feature information with category distinction is integrated into the fully connected layer, and the mapping relationship between the extracted features and sample types is constructed. The mathematical formula can be expressed as:

$$y^k = f(w^k x^{k-1} + b^k) \quad (4)$$

where k represents the network of layer k , y^k represents the output of the fully connected layer, x^{k-1} is the input of the fully connected layer, w^k is the weight coefficient, b^k represents the network offset.

Furthermore, CNN-based fault diagnosis approaches have shown promising results in accuracy and robustness. They can effectively handle large datasets and generalize to unseen data, making them suitable for real-world applications in condition monitoring and fault detection of rotating machinery systems [15] [16]. If we consider the most popular architectures among CNN for fault diagnosis of industrial machineries, SqueezeNet and ResNet18 will come into the consideration.

SqueezeNet: The SqueezeNet model minimizes the network's parameters while maintaining its classification accuracy and enhancing its training speed. This allows for better performance of the neural network model in practical applications. The main contribution of the SqueezeNet network model is the proposed Fire module, which replaces a 3×3 convolutional kernel with a 1×1 and a mixture of 1×1 and 3×3 two-layer convolutional kernels. This replacement method deepens the network depth, maintains or improves the network performance based on the original model, and reduces the number of parameters required for the model [17]. The network structure of SqueezeNet is shown in Fig 4 (a).

ResNet18: The ResNet18 is a deep neural network architecture consisting of 72 layers, with 18 being deep layers. Its design allows for the efficient functioning of numerous convolutional layers. The input size to the network is $224 \times 224 \times 3$, which is predefined. The network is considered a DAG network due to its complex, layered architecture and because the layers have input from multiple layers and give output to multiple layers [18]. In Fig 4 (b), the architecture of ResNet-18 is mentioned.

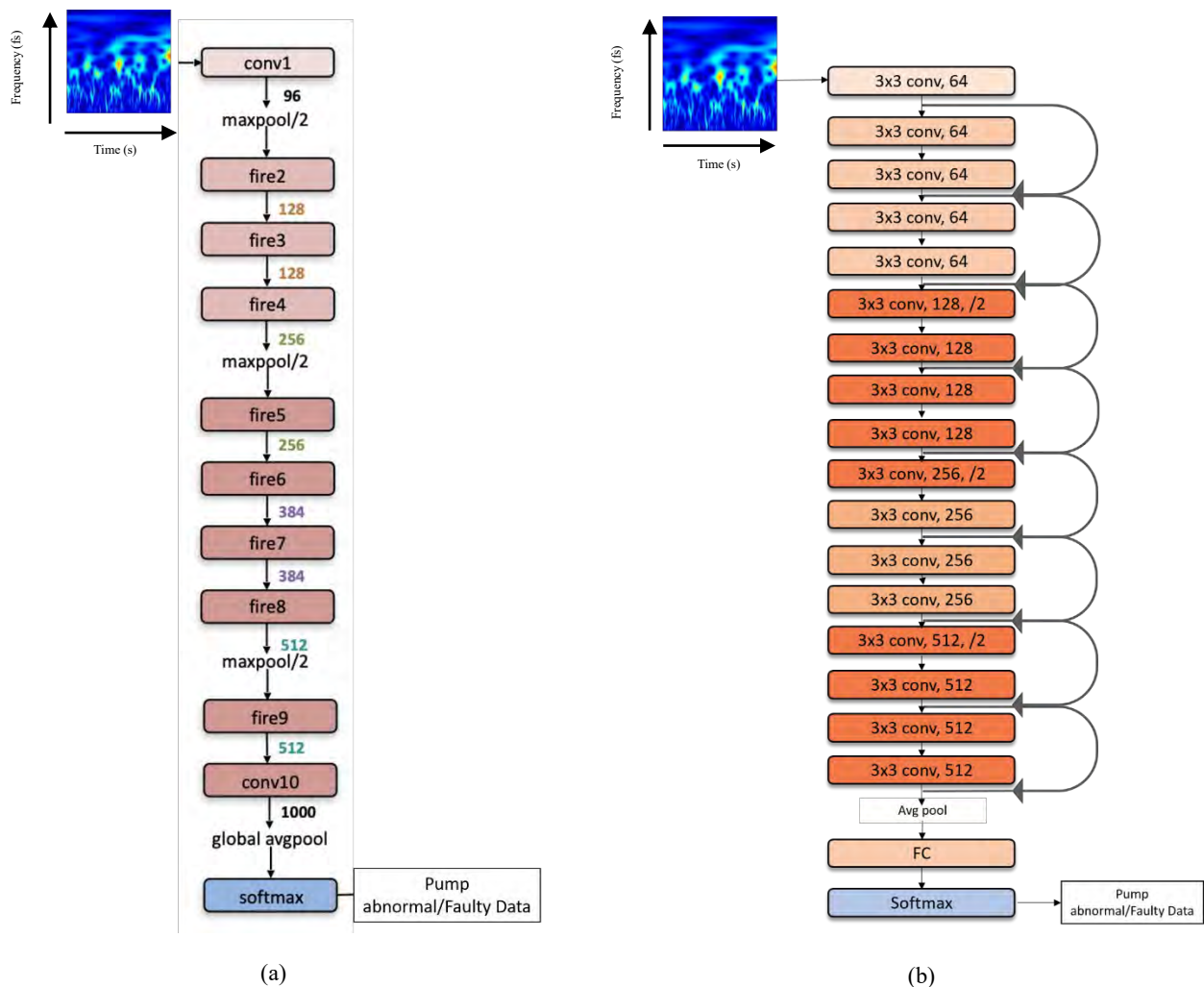


Figure 4: Network architecture of SqueezeNet (a) and ResNet-18 (b)

2.3 Activation Functions

Though CNN standard architectures have proven excellent in diagnosing machines' faults, adding multiple deep layers to a network often results in a degradation of the output. This is known as the problem of vanishing gradient where neural networks, while trained through backpropagation, rely on gradient descent, descending the loss function to find the minimizing weights [18]. The drawback of ReLU is that they cannot learn from examples for which their activation is zero. The issue often arises when ReLU is applied to the hidden layers and the neural network is initialized with all zeros. One possible reason for this is that if a ReLU neuron experiences a high gradient flow, it may update its weight and result in a negative weight and bias. If this happens, this neuron will always produce 0 during the forward propagation, and then the gradient flowing through this neuron will forever be zero, irrespective of the input [20].

In other words, the weights of this neuron will never be updated again. Such a neuron can be considered a dead neuron, a kind of permanent "brain damage" in biological terms. A dead neuron can be considered a natural Dropout [26]. However, the problem is if every neuron in a specific hidden layer is dead, it cuts the gradient to the previous layer resulting in zero gradients to the layers behind it. It can be fixed using lower learning rates, so the significant gradient does not set a considerable negative weight and bias in a ReLU neuron. Another fix is to use the Leaky ReLU, which allows the neurons outside the active interval to leak some gradient backward [19].

With the Leaky ReLU function, the accuracy of fault detection is better but increased with very small value. Another activation function is PReLU (Parametric ReLU) in which we don't multiply the negative input directly with any small value, rather we learn that small value from the training model. In feed-forward networks, each layer learns a single slope parameter. In CNNs, we can learn a separate slope parameter for each channel within each layer. The total number of slope parameters to be learned equals the sum of all channels in every layer.

Here in this paper, we have implemented modified ResNet architecture by changing the activation function with Leaky ReLU and Parametric ReLU, which successfully increased the accuracy of our experimental setup.

2.4 State of Art

Deep learning has become a vital research direction and gradually applied to various fields [a]–[d]. In [e], a dual-input model based on a convolutional neural network (CNN) and long-short term memory (LSTM) neural network has been applied. Haidong et al. [f] used a novel method called continuous deep belief network with locally linear embedding is proposed for rolling bearing fault detection. Xingqiu et al. [g] utilized modified health index based hierarchical gated recurrent unit network (GRUN) for rolling bearing health prognosis. Among them, CNN has more sophisticated applications in image processing, including image classification [h], target positioning [i], and face recognition [j]. For rolling bearing or industrial machinery fault diagnosis, scholars have provided more attention in the study of CNN architectures. Hoang et al. [k], vibration signals directly as input data, the proposed method is an automatic fault diagnosis system which does not require any additional feature extraction techniques and achieves very high accuracy. However, the above method relies on large quantities of samples that can be used for training, which is difficult to obtain in actual engineering. Moreover, in the above-mentioned CNN architectures, the issue of dead neuron exists which results in less accuracy.

Kheira et al. [i], proposed an architecture that mainly inspired by the most recent CNN models and introduce several modifications on functions and layers, such as the use of the Leaky-ReLU instead of the ReLU activation function for ECG abnormalities classification. In [j], a combination

of Leaky-ReLU activation function and three different optimizers are used that produced good and stable accuracy in the CRX and CT datasets.

Table 1: State of Art

Ref	Proposed Model	Accuracy	Limitations
[32]	The model uses both time domain and frequency domain features (TF-WConvLSTM Network) to achieve end-to-end fault diagnosis	90%+	Less recognition accuracy under strong noise
[33]	A continuous deep belief network (CDBN) is constructed based on a series of trained continuous restricted Boltzmann machines (CRBMs) to model vibration signals as a proposed model for rolling bearing fault diagnosis	91%	A prognostic system to predict the machine fault propagation trend is going to be developed further
[34]	A modified health index based hierarchical gated recurrent unit network is proposed for rolling bearing health prognosis	85%+	Health state division and failure threshold determination are both challenging yet meaningful in fault prognosis issues
[37]	Using vibration signals directly as input data, the proposed method is an automatic fault diagnosis system which does not require any feature extraction techniques and achieves very high accuracy and robustness under noisy environments.	97.74%.	Selecting appropriate hyper-parameters to design DL algorithms for fault diagnosis is still a challenge.
[35]	Proposed an architecture that mainly inspired by the most recent CNN models and introduce several modifications on functions and layers, such as the use of the Leaky-ReLU instead of the ReLU activation function for ECG abnormalities classification.	96%	the quality of this model can be enhanced by merging available datasets or creating a larger one
[36]	A combination of Leaky-ReLU activation function and three different optimizers are used that produced good and stable accuracy in the CRX and CT datasets.	97.57%	This research can be developed with a different architecture to produce better accuracy.

Considering the advantages and disadvantages of all the above work, CNN and Leaky ReLU are combined to build a deep neural network framework CNN-LR to diagnose bearing faults in this paper. This paper aims to contribute to fault diagnosis in industrial machinery by developing an

advanced and modified Transferable CNN architecture with Explainable Artificial Intelligence. The proposed system will provide accurate and interpretable fault diagnosis results, enabling timely interventions and improving industrial operations' overall reliability and efficiency [5]. In this paper, we have contributed below.

- Comparison among CNN architectures for machinery fault diagnosis.
- Modified ResNet18 architecture with activation function (Leaky ReLU)
- Implemented all three architectures in three different datasets (MFPT, MIMII, and Vehicle Engine dataset)
- We included XAI to improve the understanding of feature extraction in spectrograms for fault diagnosis.

Chapter 3

The Proposed CNN-LR Model

In this paper, a network architecture based on CNN and Leaky ReLU is established for industrial machineries fault diagnosis, which we call CNN-LR model. This chapter mainly includes the construction of CNN-LR model and industrial machine fault diagnosis based on the proposed model.

3.1 Design of CNN-LR Model

In this section, the CNN-LR model is designed, of which structure is indicated in Figure 5. The model uses transfer learning of the pre-trained ResNet-18 network to extract 2-D image features and uses the extracted features to train the model. The activation function of the architecture of ResNet-18 is replaced and modified with the Leaky ReLU function to solve the challenge of dead neurons and get better accuracy in fault diagnosis. In Fig 5 (a) the existing ResNet-18 architecture is shown and in Fig 5 (b), modified ResNet-18 is shown with Leaky ReLU Function.

In this system, the method of transfer learning in deep learning is used, and the SqueezeNet and ResNet-18 network is selected for feature extraction. The structure and parameters of both networks are shown in Table 1[17] and Table 2 [22]. Applying the relevant knowledge that has been learned in the pre-training network directly to the target field can effectively solve the problem of complicated and time-consuming manual construction of CNN and the problem of insufficient data samples obtained in actual engineering.

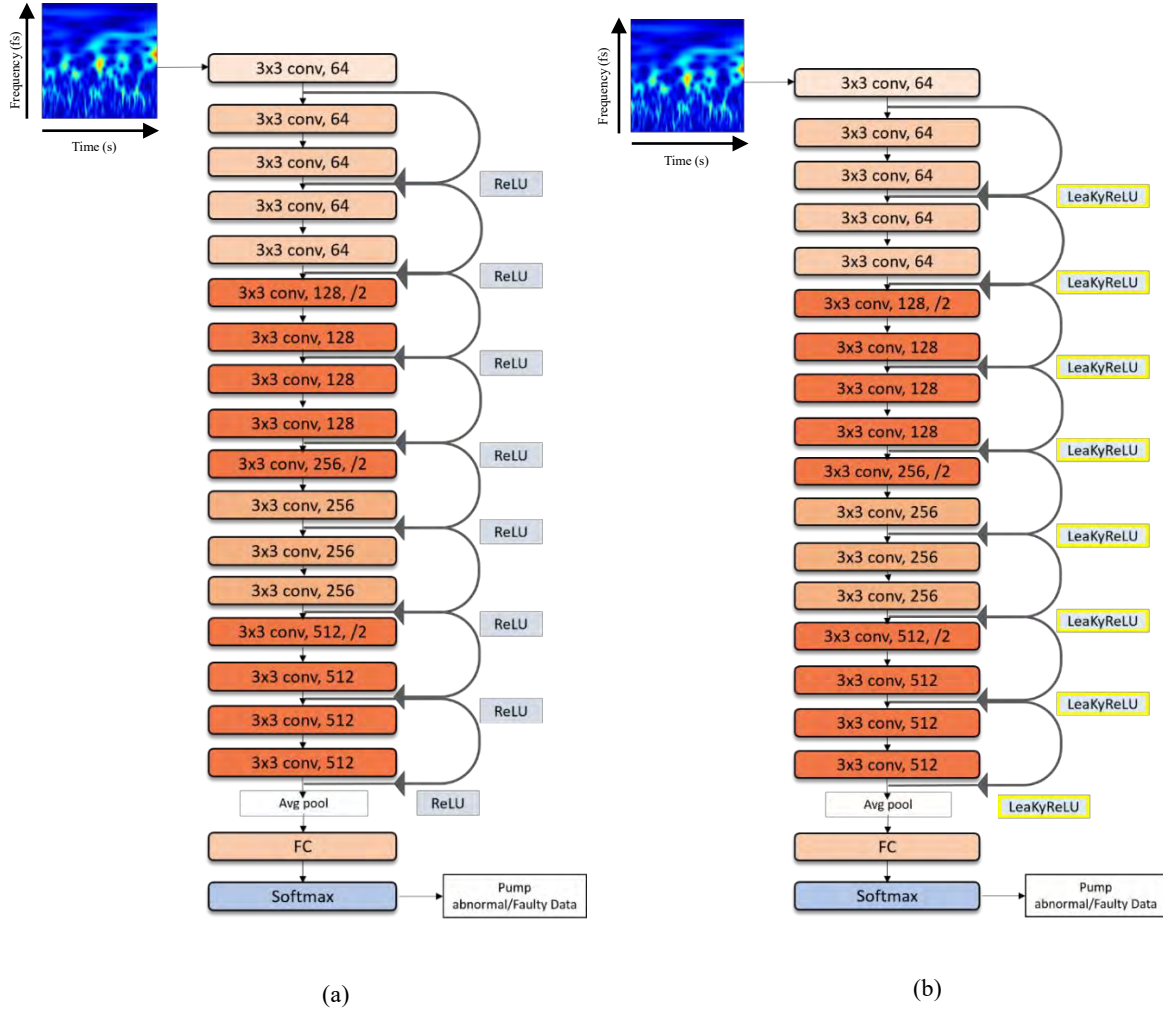


Figure 5: Network architecture of Standard ResNet-18 with ReLU activation function (a) and Modified ResNet-18 with Leaky ReLU Function (b)

Table 2: Structure and parameters of standard SqueezeNet

Layer Name	Type	Activations	Number of Learnable
Input	Image	227 x 227 x 3	
Conv1	2-D Convolution	113 x 113 x 64	1,792
Fire2/Squeeze	2-D Convolution	56 x 56 x 64	1,040
Fire2/Expand1x1	2-D Convolution	56 x 56 x 64	1,088
Fire2/Expand3x3	2-D Convolution	56 x 56 x 64	9,280
Fire3/Squeeze	2-D Convolution	56 x 56 x 16	2,064
Fire3/Expand1x1	2-D Convolution	56 x 56 x 64	1,088
Fire3/Expand3x3	2-D Convolution	56 x 56 x 64	9,280
Fire4/Squeeze	2-D Convolution	28 x 28 x 32	4,128
Fire4/Expand1x1	2-D Convolution	28 x 28 x 128	4,224

Fire4/Expand3x3	2-D Convolution	56 x 56 x 128	36,992
Fire5/Squeeze	2-D Convolution	28 x 28 x 32	8,224
Fire5/Expand1x1	2-D Convolution	28 x 28 x 128	4,224
Fire5/Expand3x3	2-D Convolution	28 x 28 x 128	36,992
Fire6/Squeeze	2-D Convolution	14 x 14 x 48	12,336
Fire6/Expand1x1	2-D Convolution	14 x 14 x 192	9,408
Fire6/Expand3x3	2-D Convolution	14 x 14 x 192	83,136
Fire7/Squeeze	2-D Convolution	14 x 14 x 48	18,480
Fire7/Expand1x1	2-D Convolution	14 x 14 x 192	9,408
Fire7/Expand3x3	2-D Convolution	14 x 14 x 192	83,136
Fire8/Squeeze	2-D Convolution	14 x 14 x 64	24,640
Fire8/Expand1x1	2-D Convolution	14 x 14 x 256	16,640
Fire8/Expand3x3	2-D Convolution	14 x 14 x 256	147,712
Fire9/Squeeze	2-D Convolution	14 x 14 x 64	32,832
Fire9/Expand1x1	2-D Convolution	14 x 14 x 256	16,640
Fire9/Expand3x3	2-D Convolution	14 x 14 x 256	147,712
conv10	2-D Convolution	14 x 14 x 1000	513,000

Table 3: Structure and parameters of standard ResNet-18

Layer Name	Type	Activations	Number of Learnable
Input	Image	224 x 224 x 3	
conv1	2-D Convolution	112 x 112 x 64	9,472
bn_conv1	Batch Normalization	112 x 112 x 64	128
pool1	2-D Max Pooling	56 x 56 x 64	
ResBlock1-1	Residual Block	56 x 56 x 64	
ResBlock1-2	Residual Block	56 x 56 x 64	
ResBlock2-1	Residual Block	28 x 28 x 128	
ResBlock2-2	Residual Block	28 x 28 x 128	
ResBlock3-1	Residual Block	14 x 14 x 256	
ResBlock3-2	Residual Block	14 x 14 x 256	
ResBlock4-1	Residual Block	7 x 7 x 512	
ResBlock4-2	Residual Block	7 x 7 x 512	
pool5	2-D Global Average Pooling	1 x 1 x 512	
fc1000	Fully Connected	1 x 1 x 1000	513,000

3.2 Proposed Method of Industrial Machine Fault Diagnosis

Industrial machinery is prone to failure or breakdown, resulting in significant company expenses. Hence, a rising interest in machine monitoring uses different sensors, including microphones. This paper presents a fault detection method for rolling bearings that utilizes CNN-LR that can take advantage of the superiority of CNN in data feature obtaining and LR's classification and generalization capabilities to solve dead neuron situations. The corresponding flow chart of the proposed method is demonstrated as Fig 6, and the steps are as follows:

Step 1:

Load three distinct experimental datasets (MFPT, MIMII, Real Dataset)

Gather vibration signals from defective bearings from each dataset

Step 2:

Function preprocess_signals(dataset):

For each dataset in (MFPT, MIMII, Real Dataset):

For each vibration signal in dataset:

Divide the vibration signal into smaller sections (A)

For each section A:

Apply Continuous Wavelet Transform (CWT) to obtain a time-frequency image

If network is SqueezeNet:

Resize the image to dimensions 227x227x3

Else if architecture is ResNet-18 or ResNet-18 LR:

Resize the image to dimensions 224x224x3

Store the time-frequency image in processed dataset

Assign a label to the time-frequency image

End For

End For

End For

Return the processed dataset

```
processed_dataset = preprocess_signals(MFPT)
```

```
processed_dataset += preprocess_signals(MIMII)
```

```
processed_dataset += preprocess_signals(Real Dataset)
```

Split processed_dataset into training samples and test samples

Step 3:

Function load_trained_CNN(network, training_samples):

Load the pre-trained CNN model 'network'

Input the training_samples into the 'network'

Obtain high-level feature representations for the training and test images

Return the trained model

Trained_Model1 = load_trained_CNN(SqueezeNet, training_samples)

Trained_Model2 = load_trained_CNN(ResNet-18, training_samples)

Trained_Model3 = load_trained_CNN(ResNet-18 LR, training_samples)

Trained_Model4 = load_trained_CNN(ResNet-18 PR, training_samples)

Step 4:

Function validate_fault_diagnosis(test_samples, models):

For each model in models:

 Input the test_samples into the model

 Obtain predictions for fault diagnosis

Return the predictions from all models

test_samples = preprocess_signals(Test Dataset)

models = [Trained_Model1, Trained_Model2, Trained_Model3, Trained_Model4]

results = validate_fault_diagnosis(test_samples, models)

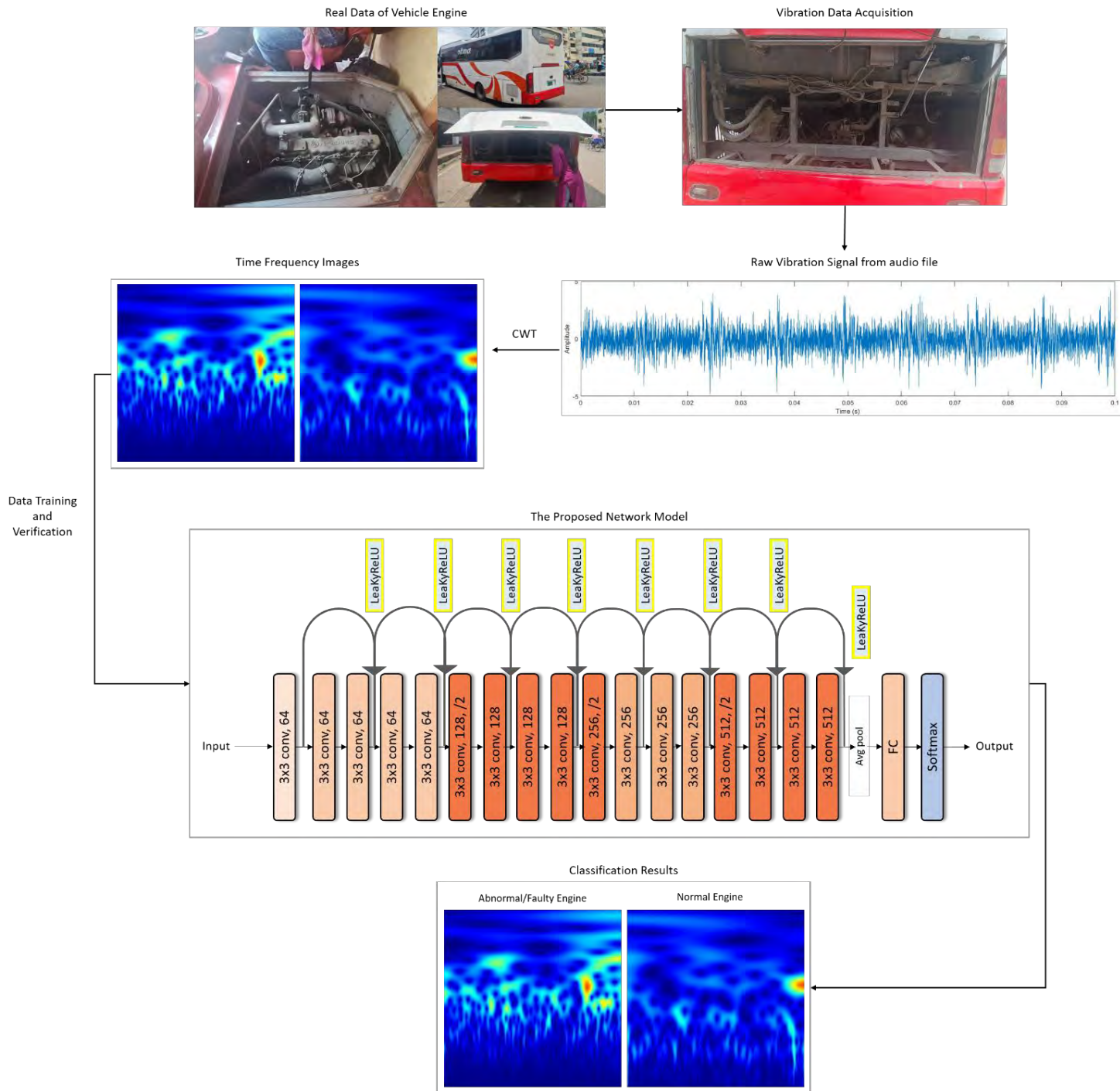


Figure 6: The flowchart of experiment

Chapter 4

Experimental Setup

We must test the flexibility and usefulness of the model we built for diagnosing bearing faults. For that, two open-source datasets are used for research in this paper, including Mechanical Failure Prevention Technology (MFPT) dataset [9] and Malfunctioning Industrial Machine Investigation and Inspection (MIMII) Dataset [23]. Besides the open-source datasets, the proposed model experimented with the real dataset of transportation buses of a Bangladeshi Transportation company called Saintmartin Travels [24].

4.1 MFPT Dataset

4.1.1 Data Description

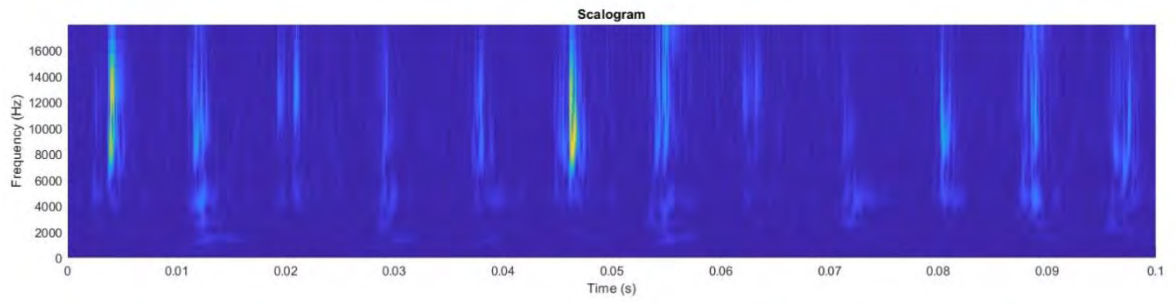
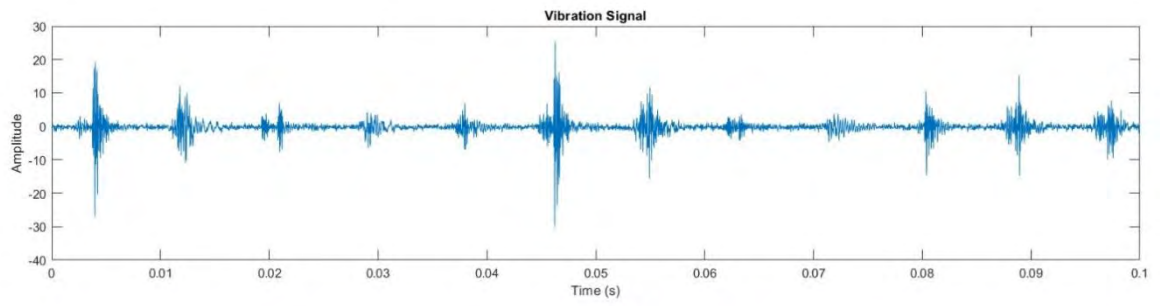
The MFPT Challenge data [9] includes a dataset of bearing faults used for research on bearing analysis. The dataset consists of three real-world faults, which include nominal bearing data, an outer race fault at various loads, and an inner race fault at various loads. The baseline dataset comprises three files, each containing data sampled at 97656 Hz for 6 seconds under a 270-pound load. The inner race fault dataset contains seven files, which are respectively obtained by sampling at 48828 Hz for 3 seconds under seven load conditions, including 0, 50, 100, 150, 200, 250, and 300 pounds. The outer race fault dataset contains seven files, which are respectively obtained by sampling at 48828 Hz for 3 seconds under seven load conditions, including 25, 50, 100, 150, 200, 250, and 300 pounds. The data points are from a single-channel radial accelerometer. The experiment bearings of the MFPT data set are also deep groove ball bearing with a 31.62 mm pitch diameter, a 5.97 mm ball diameter, a 0° contact angle, and an element number of 8. This study selects the three sets of bearing vibration data collected at the test rig.

4.1.2 Data Processing

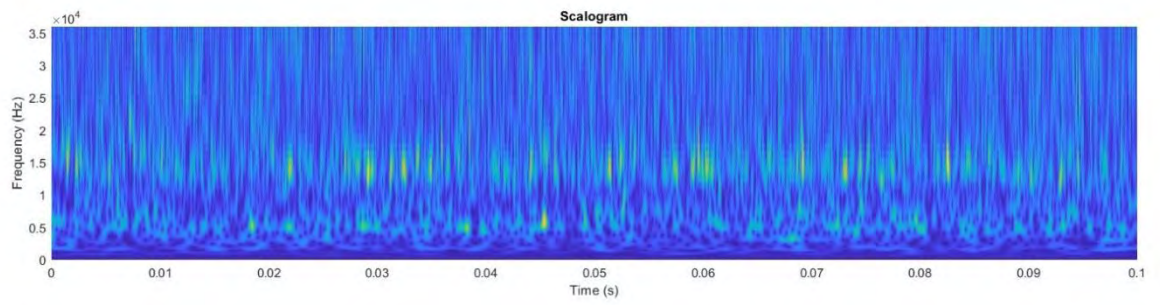
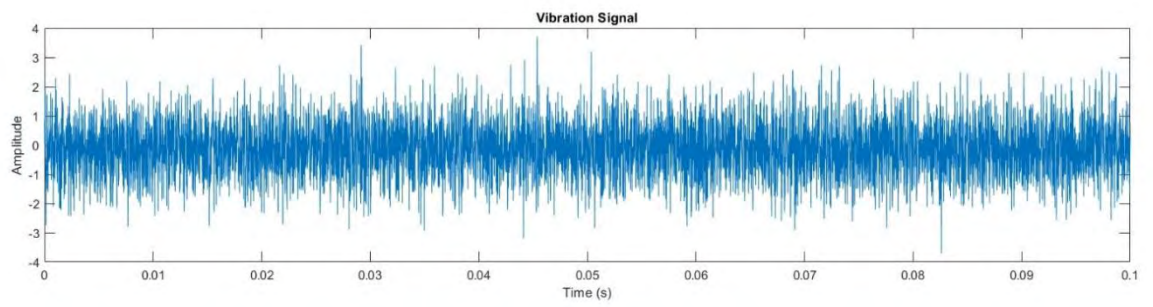
For this experiment, we used all the data points from the three fault data sets and selected a sample length 48828. We repeated 24414 data points between adjacent parts to increase the number of experimental samples. The baseline set is down sampled to 48828 Hz to match other fault sets. The three files in the baseline set are divided into 22 segments, respectively; the seven inner fault files are divided into five segments, respectively; and the seven external fault files are divided into five segments. Through the CWT [7], a corresponding number of time-frequency images in each state can be obtained. By merging the load conditions under the three fault types, 66 time-frequency images for the baseline set, 35 time-frequency images for the inner race, and 35 time-frequency images for the outer race are obtained. Finally, a sample set containing 136 time-frequency images is obtained, as shown in Table 3. According to [5], 80% of each state's images are selected randomly for training, while the remaining 20% are reserved for testing. In Fig. 7 (a)-(c), the time-frequency images of the three health conditions in Table 3 are shown in sequence.

Table 4: The sample description of MFPT dataset

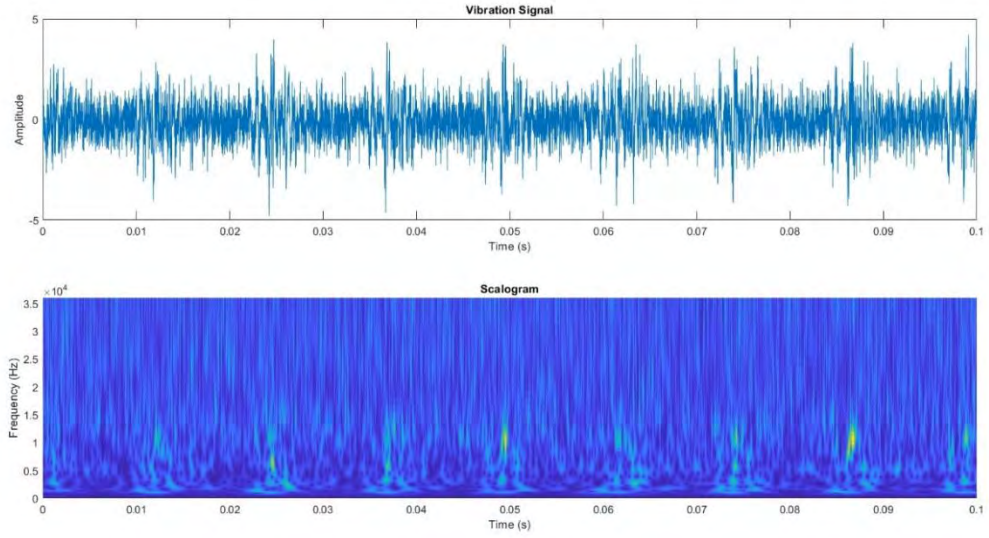
Class Type	Load (lb)	Number of files	Input Shaft Rate	Sample Rate
Baseline condition	270	3	25 Hz	97,656 sps
Outer race fault condition	25, 50, 100, 150, 200, 250, 270, 270, 270, 300	10	25 Hz	48,828 sps
Inner race fault condition	0, 50, 100, 150, 200, 250, 300	7	25 Hz	48,828 sps



(a)



(b)



(c)

Figure 7: Time-frequency images of three health conditions on MFPT dataset: (a) Baseline; (b) Outer; (c) Inner.

4.1.3 Results of the Experiment

We first train the CNN-LR model using the training samples we constructed for the three bearing fault types. The Training time is 12 minutes and 2 seconds which was done on 164 samples. The details of the training progress are shown in Fig 8. Upon completion of the training, the model must be verified using the test sample. This experiment is implemented in three architectures of CNN. With the model SqueezeNet, the fault diagnosis classification accuracy is 94.64%; with ResNet-18, the accuracy is 94.42%; and with our proposed model CNN-LR and CNN-PR, the fault diagnosis classification accuracy is 96.57% and 97.99% respectively. Table 4 shows the values of detailed information of three networks with respective Training Accuracy, Training Loss, Validation Accuracy, and Validation Loss for the MFPT dataset.

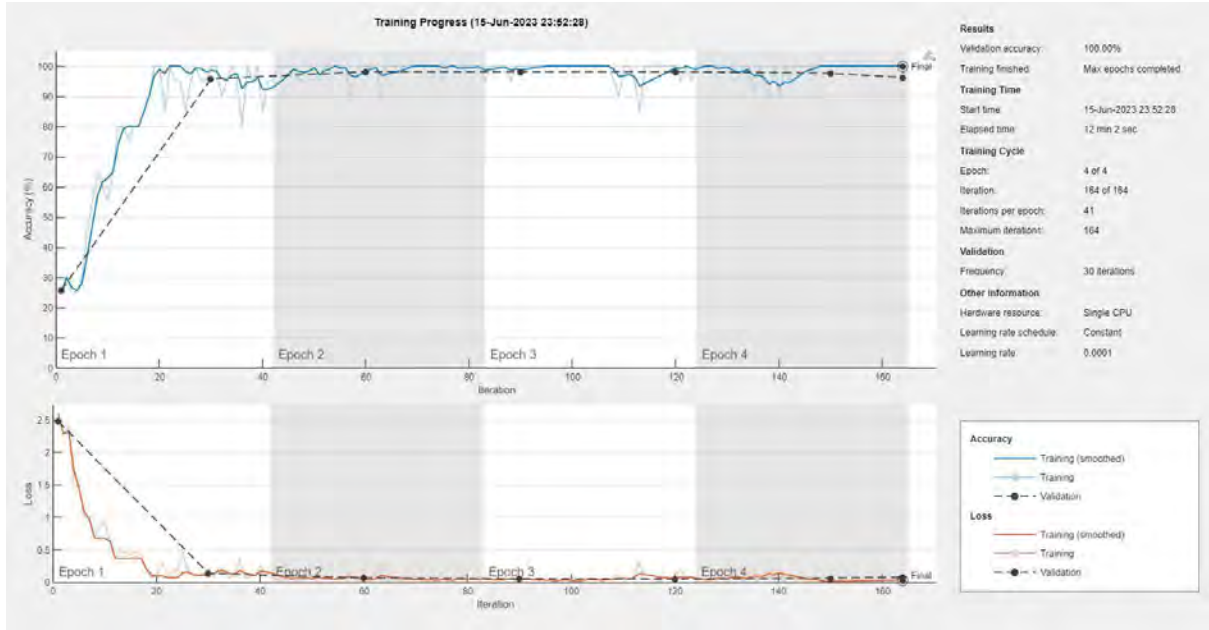


Figure 8: Training Progress of CNN_LR model of MFPT Dataset

Table 5: Accuracy Comparison between Standard SqueezeNet, Standard ResNet-18, proposed CNN-LR model and proposed CNN-PR model

MFPT Dataset				
Network Name	Standard SqueezeNet	Standard ResNet18	Proposed Model with LR	Proposed Model with PR
Status	Complete (Max epochs completed)	Complete (Max epochs completed)	Complete (Max epochs completed)	Complete (Max epochs completed)
Progress	<div style="width: 100%; height: 10px; background-color: #90EE90;"></div>	<div style="width: 100%; height: 10px; background-color: #90EE90;"></div>	<div style="width: 100%; height: 10px; background-color: #90EE90;"></div>	<div style="width: 100%; height: 10px; background-color: #90EE90;"></div>
Elapsed Time	5 min 19 sec	11 min 54 sec	12 min 2 sec	10 min 8 sec
Training Accuracy	91.62%	95.06%	93.72%	95.07%
Training Loss	0.2238	0.145	0.1723	0.1143
Validation Accuracy	98.57%	99.52%	100.00%	100.00%
Validation Loss	0.0336	0.0272	0.0214	0.0187
Fault Detection Accuracy for Industrial Machineries	94.64%	94.42%	96.57%	97.99%

The confusion matrix [25] of three experimented models is also shown in Fig 9 (a) – (d) which are representing the prediction summary in matrix form. It shows how many predictions are

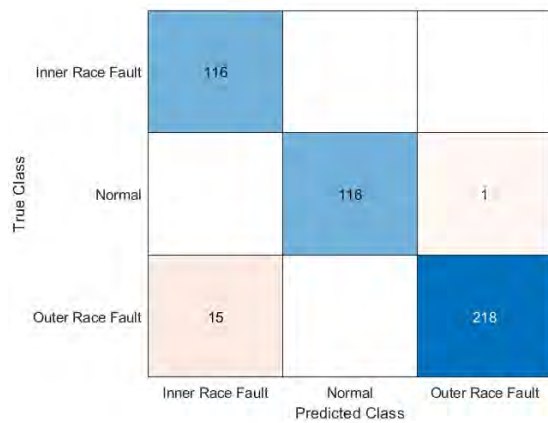
correct and incorrect per class. It helps in understanding the classes that are being confused by model as other class.



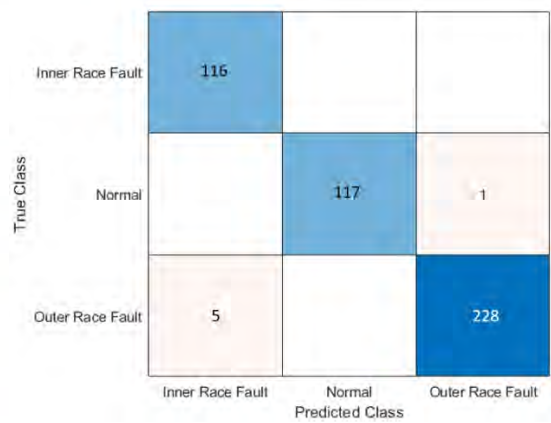
(a)



(b)



(c)



(d)

Figure 9: Confusion matrix of MFPT dataset for (a) Standard SqueezeNet; (b) Standard ResNet-18 and (c) CNN-LR Model (d) CNN-PR Model

4.2 MIMII Dataset

4.2.1 Data Description

The MIMII dataset is a collection of sound recordings that can be used to investigate and inspect malfunctioning industrial machines [23]. The dataset includes sounds from four types of machines: valves, pumps, fans, and slide rails. Each machine type has seven different models*1, and for each model, there are recordings of normal sounds (from 5000 seconds to 10000 seconds) and anomalous sounds (about 1000 seconds). Normal and anomalous sounds were recorded for different types of industrial machines. Also, the background noise recorded in multiple real factories was mixed with the machine sounds. The sounds were recorded by an eight-channel microphone array with a 16 kHz sampling rate and 16 bits per sample. This dataset contains the sound of four different types of machines: valves, pumps, fans, and slide rails. The valves are solenoid valves that are repeatedly opened and closed. The pumps are water pumps that drain water from a pool and continuously discharge water to the pool. The fans represent industrial fans, providing a continuous air flow in factories. The slide rails in this paper represent linear slide systems, which consist of a moving platform and a staging base. The list of sound files for each machine type is mentioned in Table 5. Each type of machine consists of seven individual machines. This dataset contains 26,092 sound segments of normal conditions and 6,065 sound segments of anomalous conditions.

Table 6: MIMII dataset content details

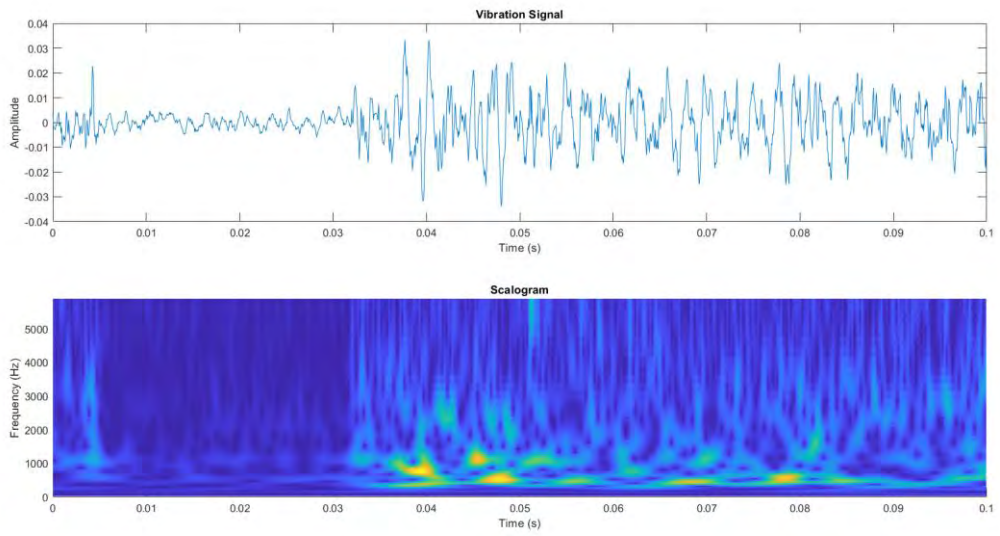
Machine type	Model ID	Segments for Normal Condition	Segments for anomalous condition
Valve	00	991	119
	01	869	120
	02	708	120
	03	963	120
	04	1000	120
	05	999	400
	06	992	120
Pump	00	1006	143
	01	1003	116
	02	1005	111
	03	706	113
	04	702	100
	05	1008	248
	06	1036	102
Fan	00	1011	407
	01	1034	407
	02	1016	359
	03	1012	358
	04	1033	348
	05	1109	349
	06	1015	361
Slide rail	00	1068	356
	01	1068	178
	02	1068	267
	03	1068	178
	04	534	178
	05	534	178
	06	534	89
Total		26092	6065

4.2.2 Data Processing

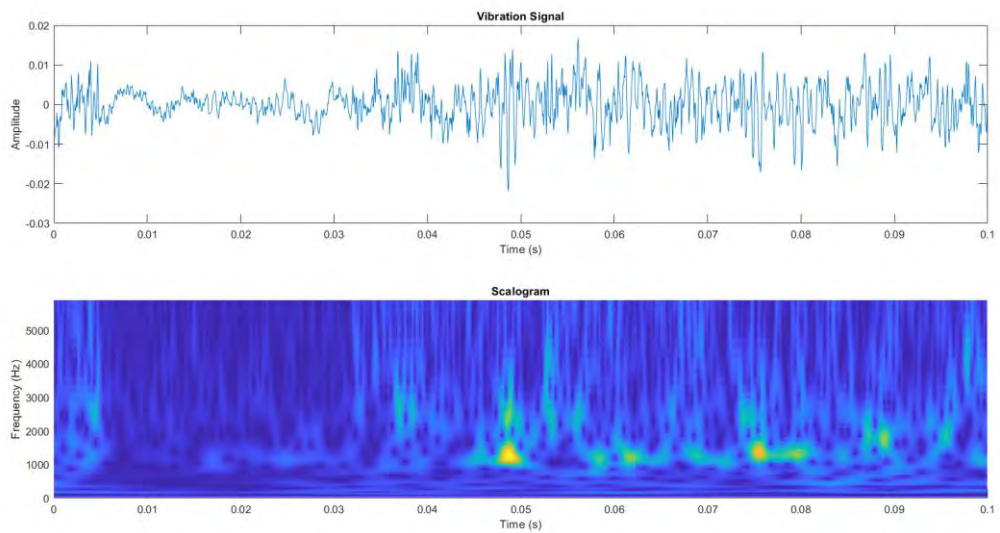
We have taken the samples from the segment pump, fan, slider and valve with two classes for the MIMII Data processing. The normal sound dataset of the all categories is 2048 Kbps, and the abnormal or faulty dataset is 2048 Kbps. First, we processed the audio files through CWT [6] [7] to get a corresponding number of time-frequency images for each condition. By merging the load conditions under the two class types, 3124 time-frequency images for the normal dataset of each category and 3124 time-frequency images for the abnormal dataset of the each category were obtained. Finally, a sample set containing 1562 time-frequency images is obtained, as shown in Table 6. Among them, 80% of the images in each state are randomly chosen as training samples, and the remaining 20% are used as test samples. In Fig. 10 (a)-(b), the time-frequency images of the Fan class of MIMII dataset in Table 6 are shown in sequence.

Table 7: Detail data of selected MIMII dataset file

Class Type	Bit rate	Number of files	File type	Duration of each file
Pump_Abnormal	2048 Kbps	30	WAV	10 sec
Pump_Normal	2048 Kbps	30	WAV	10 sec
Fan_Abnormal	2048 Kbps	30	WAV	10 sec
Fan_Normal	2048 Kbps	30	WAV	10 sec
Slider_Abnormal	2048 Kbps	30	WAV	10 sec
Slider_Normal	2048 Kbps	30	WAV	10 sec
Valve_Abnormal	2048 Kbps	30	WAV	10 sec
Valve_Normal	2048 Kbps	30	WAV	10 sec



(a)



(b)

Figure 10: Time-frequency images of three health conditions on MIMI dataset: (a) Abnormal pump dataset (b) Normal pump dataset

4.2.3 Results of the Experiment

With MIMII dataset, we have followed the same procedures and that is our approached model CNN-LR is trained with the samples of two class of pump dataset. Here, we have done the training with total 996 samples and the total training time is 117 minutes 50 seconds. The hardware specification is Windows 11, 64 bit operating system, Intel(R) Core(TM) i5-8265U CPU @ 1.60GHz, 1.80 GHz. The details of training progress are shown in Fig 11. The trained model is verified by the test sample after completion of training progress. This experiment is also tested over three architectures of CNN. With the model SqueezeNet, the fault diagnosis classification accuracy is 89.12% 9 (avg), with ResNet-18, the accuracy is 94.56% (avg) and with our proposed model CNN-LR and CNN-PR, the fault diagnosis classification accuracy is 95.33% and 96.50% (avg). In Table 7, the values of detail information of three networks are shown with respective Training Accuracy, Training Loss, Validation Accuracy and Validation Loss for MFPT dataset.

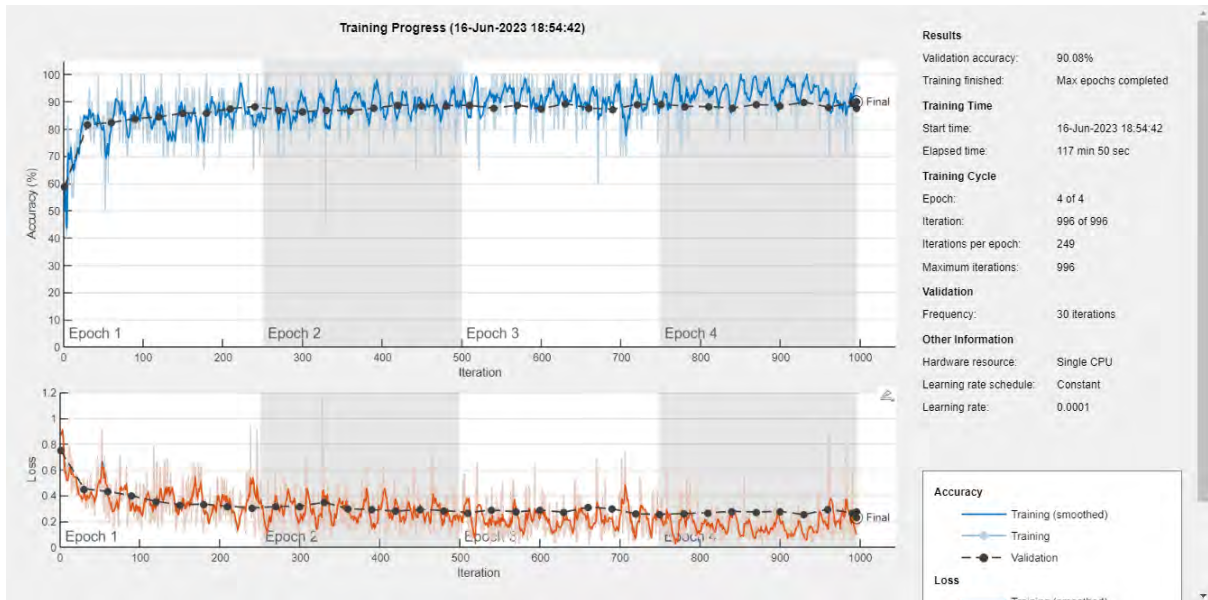






Figure 11: Training Progress of CNN_LR model of MIMII Dataset

Table 8: Accuracy Comparison between Standard SqueezeNet, Standard ResNet-18 and proposed CNN-LR model of MIMII dataset

MIMII Dataset (on average)				
Network Name	Standard SqueezeNet	Standard ResNet18	Proposed CNN-LR	Proposed CNN-LR
Status	Complete (Max epochs completed)	Complete (Max epochs completed)	Complete (Max epochs completed)	Complete (Max epochs completed)
Progress	 100%	 100%	 100%	 100%
Elapsed Time	44 min 56 sec	117 min 50 sec	109 min 32 sec	102 min 04 sec
Training Accuracy	88.04%	89.08%	89.13%	90.41%
Training Loss	0.2916	0.2637	0.2596	0.1542
Validation Accuracy	90.08%	91.76%	90.08%	92.16%
Validation Loss	0.2393	0.2187	0.2333	0.1928
Fault Detection Accuracy for Industrial Machinerics	89.12%	94.56%	95.33%	96.50%

For the MIMII dataset, at first we have identified the type of machine with the sound type in Fig 12, and then again run the same approach to identify whether that identified machine is faulty or not. Below are the images of Confusion Matrix for identifying the machine type with three architectures.

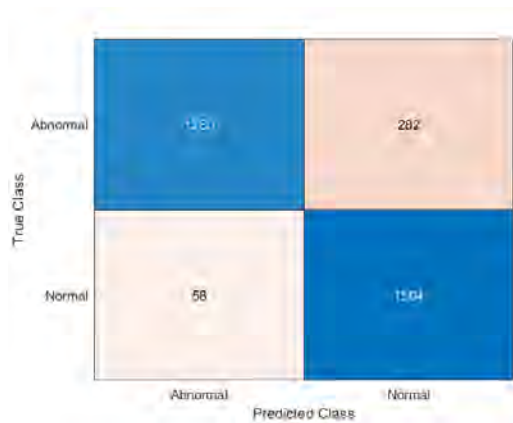


True Class	Pump	5876	128	110	134
	Fan	95	5654	289	210
	Slider	102	69	6003	74
	Valve	198	55	166	5829
		Pump	Fan	Slider	Valve
		Predicted Class			

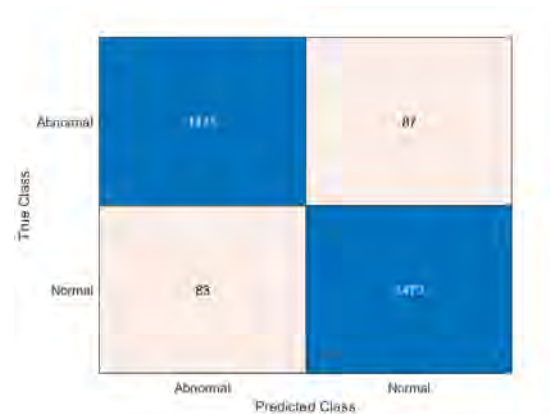
(c)

Figure 12 Confusion matrix of MIMII dataset four types of machine identification for (a) Standard SqueezeNet; (b) Standard ResNet-18 and (c) Proposed CNN-LR Model

In Fig 13, the confusion matrix of three experimented models is also shown to have summary in matrix form. It clearly represents correct and incorrect prediction per class similarly like MFPT dataset [25].



(a)



(b)

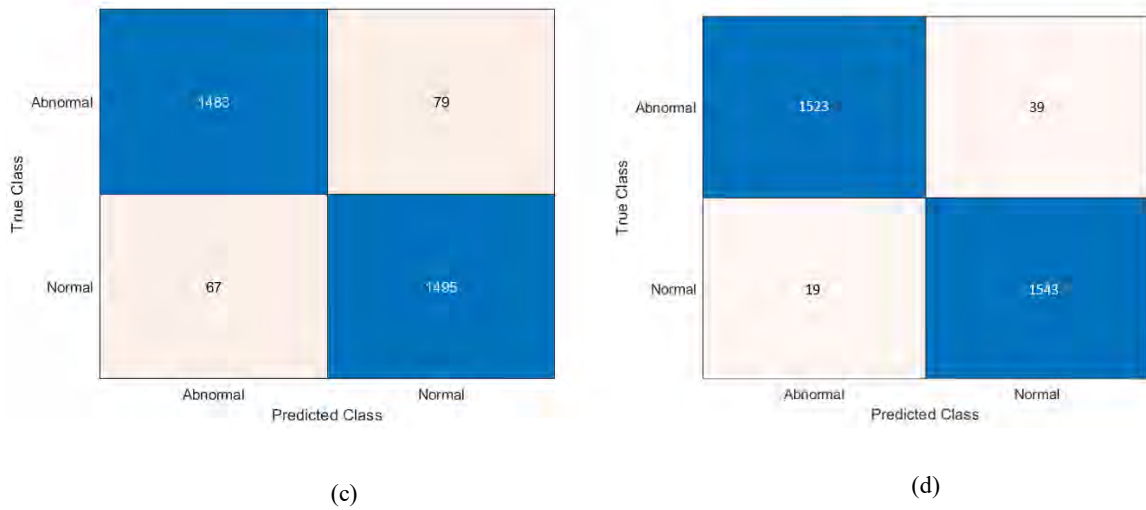


Figure 13: Confusion matrix of MIMII dataset for (a) Standard SqueezeNet; (b) Standard ResNet-18; (c) Proposed CNN-LR Model and (d) Proposed CNN-PR Model

4.3 Vehicle Engine Dataset

4.3.1 Data Description

We have applied our model to a real dataset of vehicle engines for the third dataset. Vehicle engine faults refer to significant issues that arise within a vehicle's engine. Due to their intricate structure and running conditions, engine faults are responsible for approximately 40 percent of all vehicle failures. Here, we have collected the raw audio data of a new transport bus, which is later defined as the normal sound of a vehicle engine, and also collected raw audio data of an old transport bus with a small number of faulty engines, defined as the abnormal sound of the vehicle engine. The sounds were recorded by the Voice Recorder App of the Samsung Note 20 handset. In Table 8, the details of the vehicles for both normal and abnormal vehicle engine sound is mentioned. The actual data on normal and faulty engines is collected from a transportation company in Bangladesh called Saintmartin Travels [24]. The approval for using the data in this research is shared in

Appendix 1. The reference images of the bus engines while recording the sound are shared in Fig 14.

Table 9: Vehicle details from which sample data collected

Faulty engine transport bus	
Bus Model	ISUZU 36 Seater
Seating Capacity	36+D (2x2 Fix)
Engine	SLTHT6 CRDI TCIC, 3455 cc
Power	114 HP @ 2600 rpm
Torque	400 Nm @ 1400-1600 rpm
Fuel	Diesel
Cylinders	4



(a)



(b)



(c)



(d)



(e)



(f)

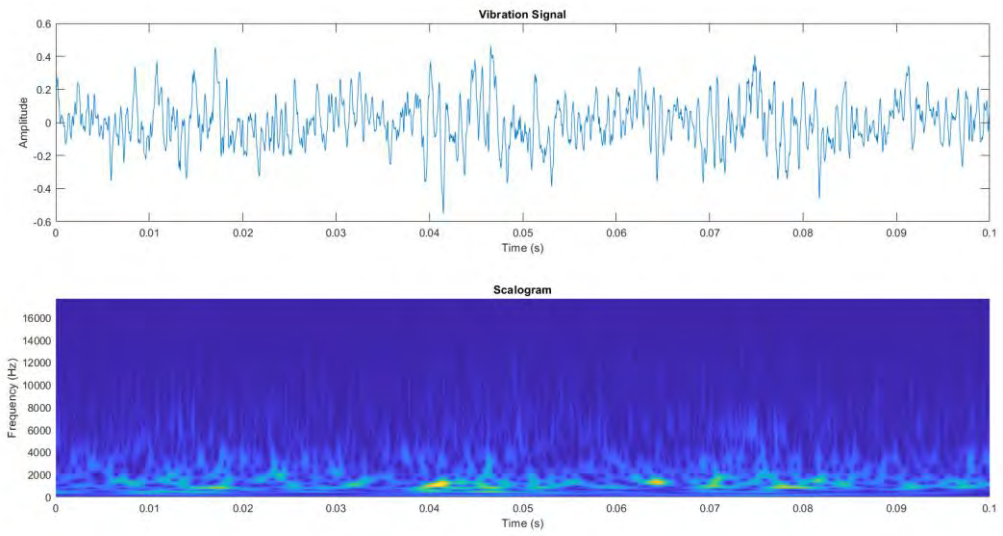
Figure 14: Images of Transport Vehicle of Saintmartin Travels; (a) Normal/new sleeper coach, (b) Engine of normal/new sleeper coach, (c) Faulty/Old bus, (d) Engine of faulty/old bus, (e) taking sample of engine sound and (f) Photo with Director of Saintmartin Travels

4.3.2 Data Processing

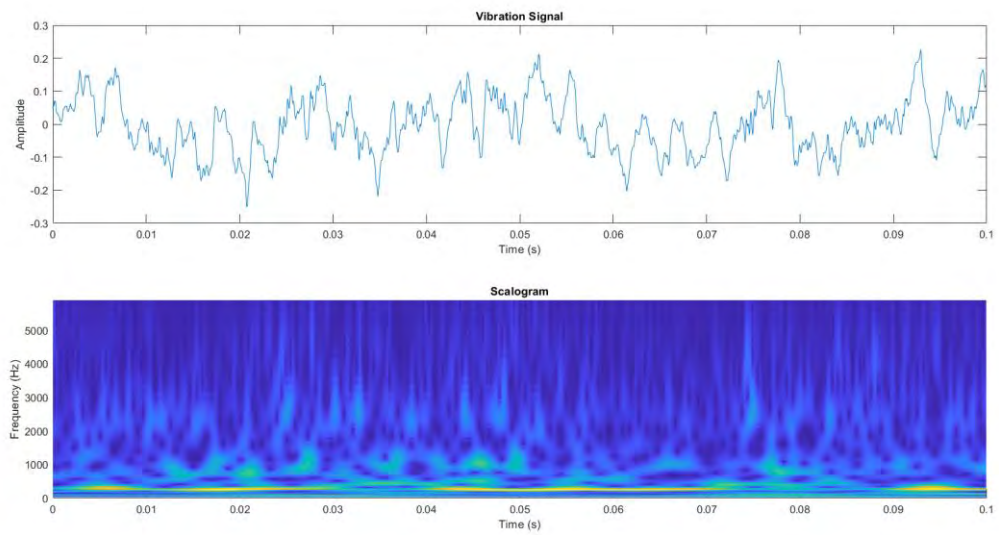
In this experiment, five audio files are collected from each vehicle for both normal engine sound and abnormal engine sound. Each data group has been divided into 1562 time-frequency images through CWT. Among them, 80% of the images under each class type are randomly chosen as training samples, and the remaining 20% are used as test samples [5]. In Fig. 15 (a)-(b), the time-frequency images of both the vehicle engine in Table 9 are shown in sequence.

Table 10: The sample description of Vehicle Engine dataset

Class Type	Bit rate	Number of files	File type	Duration of each file
Vehicle_Engine_Abnormal	252 kbps	10	WAV	10 sec
Vehicle_Engine_Normal	252 kbps	10	WAV	10 sec



(a)



(b)

Figure 15: Time-frequency images of two classes on Vehicle Engine dataset: (a) Abnormal vehicle engine dataset (b) Normal vehicle engine dataset

4.3.3 Results of the Experiment

With the real vehicle engine dataset, we have followed the same procedures as the other two datasets. Firstly, CNN-LR is trained with the samples of two classes of vehicle engine datasets. Here, we have done the training with a total of 996 samples, and the total training time is 109 minutes 32 seconds. The hardware specification is the same as other datasets for training. The details of the training progress are shown in Fig 16. The test sample verifies the trained model after completing the training progress. This experiment is also tested over three architectures of CNN. With the model SqueezeNet, the fault diagnosis classification accuracy is 89.12%. With ResNet-18, the accuracy is 92.91%, and with our proposed model CNN-LR and CNN-PR, the fault diagnosis classification accuracy is 94.56% and 96.21% respectively. In Table 10, the values of detail information of three networks are shown with respective Training Accuracy, Training Loss, Validation Accuracy, and Validation Loss for real datasets of vehicle engines.

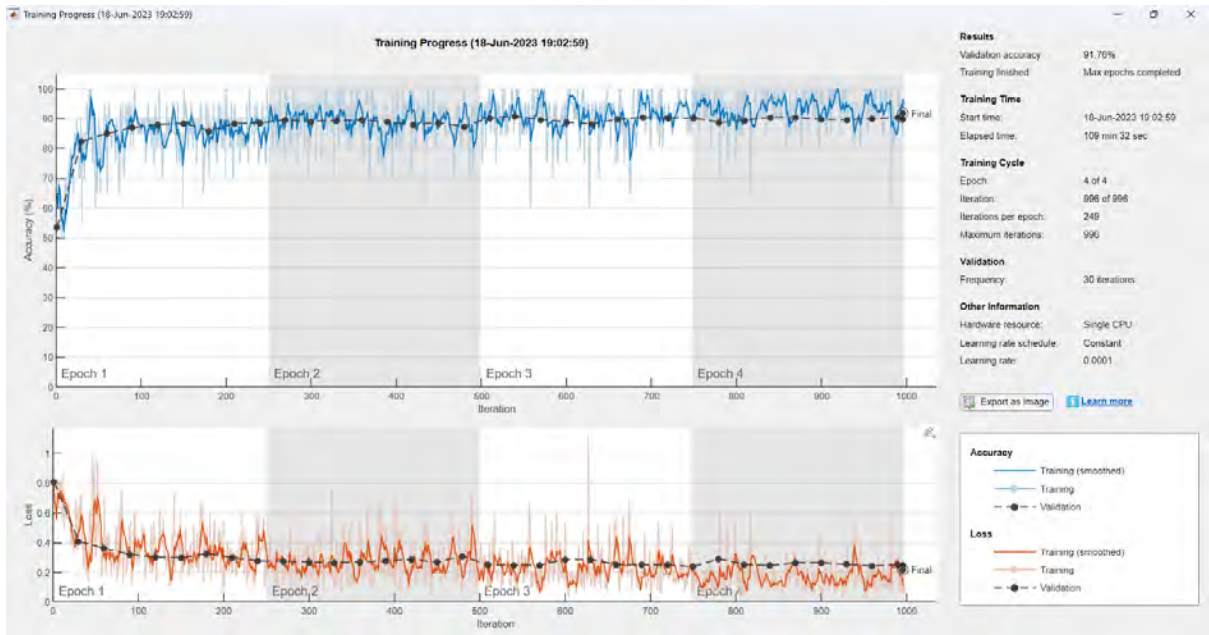




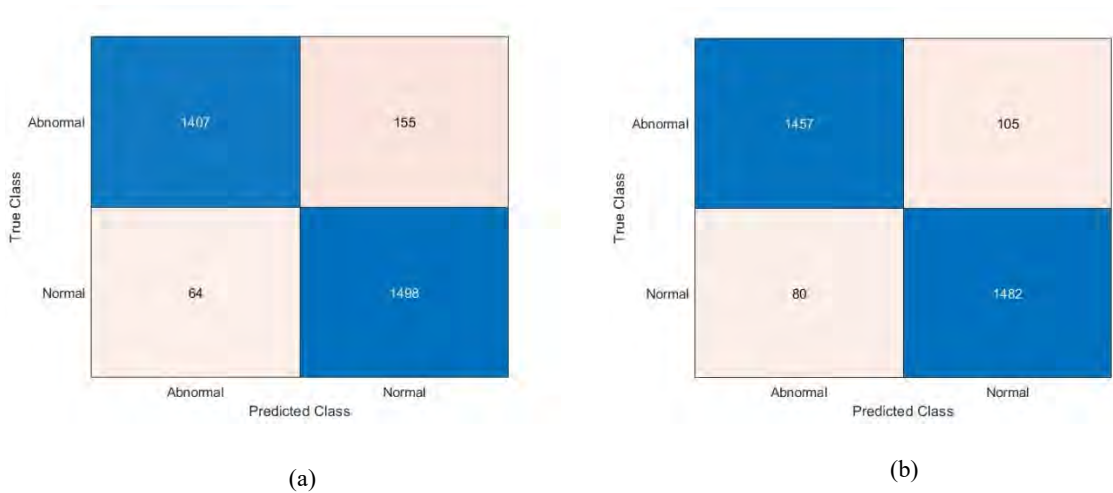


Figure 16: Training Progress of CNN_LR model of Vehicle Engine Dataset

Table 11: Accuracy Comparison between Standard SqueezeNet, Standard ResNet-18 and proposed CNN-LR model of Vehicle Engine dataset

Vehicle Engine Dataset				
Network Name	Standard SqueezeNet	Standard ResNet18	Proposed CNN-LR	Proposed CNN-PR
Status	Complete (Max epochs completed)	Complete (Max epochs completed)	Complete (Max epochs completed)	Complete (Max epochs completed)
Progress	 100%	 100%	 100%	 100%
Elapsed Time	124 min 41 sec	110 min 27 sec	109 min 32 sec	121 min 54 sec
Training Accuracy	88.04%	88.59%	89.08%	92.17%
Training Loss	0.2916	0.2659	0.2637	0.2532
Validation Accuracy	90.08%	91.04%	91.76%	93.19%
Validation Loss	0.0105	0.2253	0.2187	0.2014
Fault Detection Accuracy for Industrial Machineries	89.12%	92.91%	94.56%	96.21%

In Fig 17, the confusion matrix [25] of three experimented models is also shown to have summary in matrix form. It clearly represents correct and incorrect prediction per class similarly like MFPT dataset and MIMII dataset.



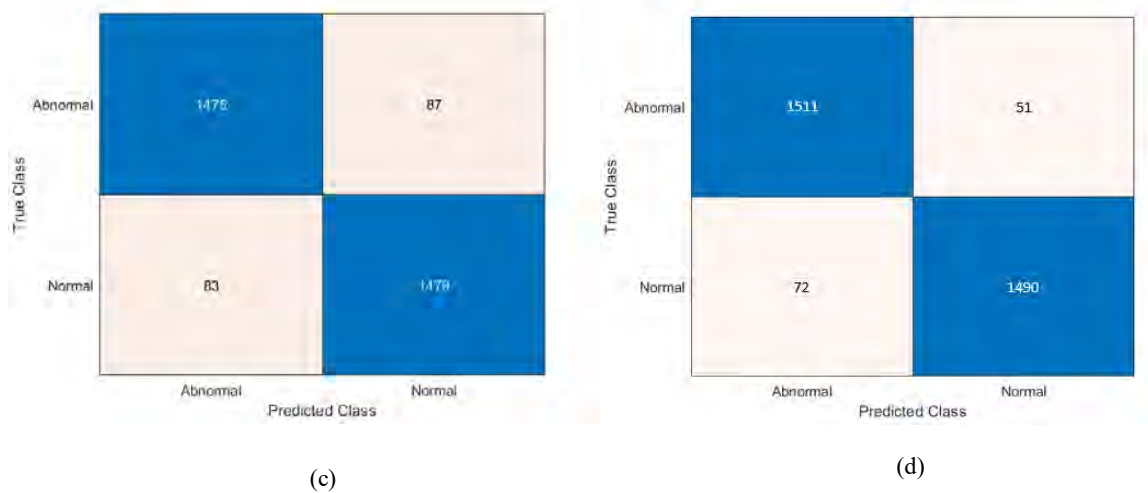


Figure 17: Confusion matrix of Vehicle Engine dataset for (a) Standard SqueezeNet; (b) Standard ResNet-18; (c) Proposed CNN-LR Model and (d) Proposed CNN-PR Model

4.4 Explainable Artificial Intelligence (XAI)

Explainable Artificial Intelligence (XAI) is an essential concept of machine learning that aims to explain how machine learning models generate outputs. Incorporating XAI into a machine learning model makes the model more dependable since we can monitor the model's inference process. There are some already established methods for CNN.

Lime: The model employed by the system is designed for easy comprehension and can learn from examples in a specific region.

Grad-Cam: This tool utilizes counterfactual explanations to modify CNN predictions and can explain all layers, including the final hidden layer.

In Fig 18, the comparison of LIME and Grad-Cam is mentioned. Here we have chosen input images from every class of our three datasets. For the MFPT dataset, we have taken three input

images from the inner race, outer race, and baseline, respectively. Normal and abnormal pump spectrogram images are taken for XAI for the MIMMI dataset. Moreover, finally, for our real dataset, we have taken faulty and normal engine spectrogram images [3].

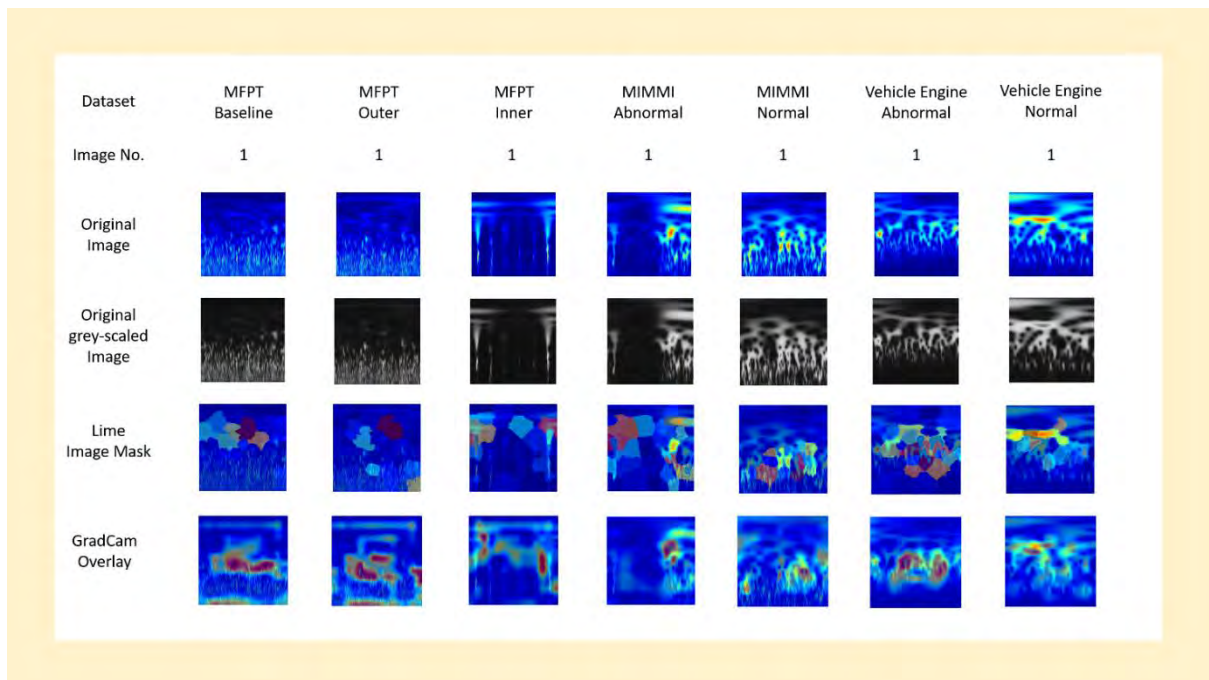


Figure 18: Comparison of XAI methods on MFPT, MIMMI and Vehicle Engine datasets

4.5 Result Analysis

To prove the better accuracy of the proposed model, we have compared it with standard CNN architectures. The inputs of SqueezeNet and ResNet-18 architectures are also the time-frequency images. In order to ensure the fairness of the experiment and the reliability of the results, the whole test is repeated five times on these two existing architectures by using the MFPT dataset, MIMII dataset and Real dataset. The diagnosis accuracy of each method is shown in Fig. 19. The diagnosis accuracy and average training time of the three methods are summarized in Table 11.

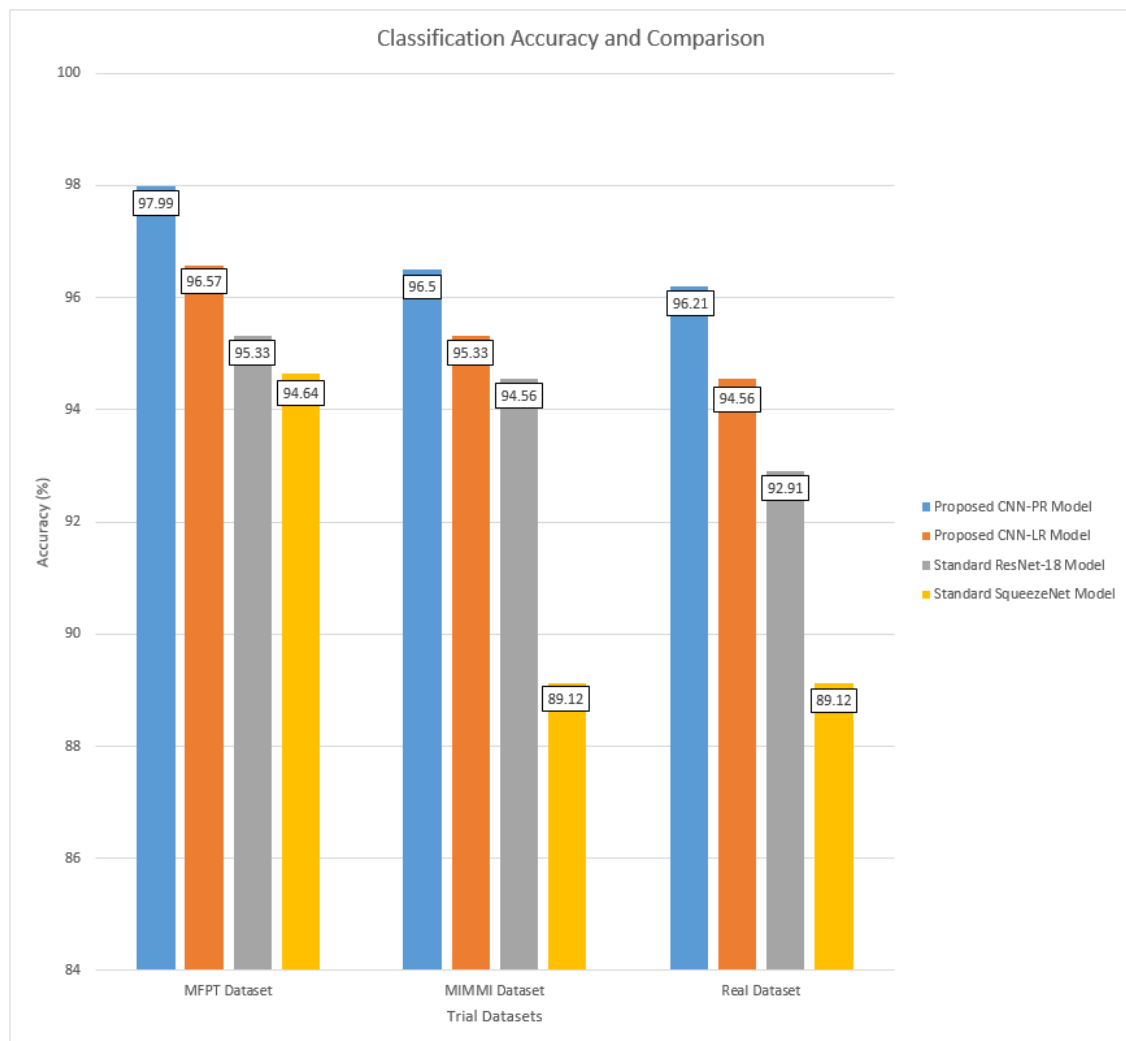


Figure 19: Classification accuracy and comparison of four different CNN models on three different datasets

Table 12: Average accuracy and average training time of four CNN models

Models	Average Accuracy (%)	Average Training Time (s)
Proposed Architectures (on avg)	95.49	4622.00
Standard ResNet-18	93.96	4803.67
Standard SqueezeNet	90.96	3498.67

As we can see, the fault diagnosis accuracy of the proposed method in three different datasets is higher than that of the other two standard CNN architectures. The results show that if we use the existing CNN network architecture and if we replace the existing ReLU function with Leaky ReLU and Parametric ReLU, it provides better accuracy. It is proved that the proposed model can effectively solve the difficult situation of Dead Neuron of deep learning network.

By comparing the results with other methods, it can be easily seen that the proposed method achieves a higher diagnosis accuracy, which further shows the effectiveness of the proposed method.

Chapter 5

Conclusion and Future Work

In this study, a new deep neural network model CNN-LR is built for fault diagnosis of industrial machinery. First, we use the CWT to construct the time-frequency images of vibration signals. Then, the obtained images are input into the proposed model for training. Finally, the diagnosis of the fault location and severity of the industrial machinery is completed. The experiments indicate that the diagnostic accuracy of this method can reach 96.57% for the MFPT dataset, 95.33% for the MIMII dataset, and 94.56% for the Vehicle engine dataset, which verifies the flexibility and practicability of the constructed model. By comparing with the standard SqueezeNet and standard ResNet-18, it is shown that the proposed model can resolve the difficulty of deep feature extraction in the traditional method and the dead neuron problem in existing architectures. We have deployed XAI functions that can show how the CNN model predicts the image class and identifies which parts of the image have the most significant impact on the CNN model's final prediction.

However, for relatively noisy data sources, the accuracy of the proposed method still needs to be enhanced. Therefore, the structure of the proposed model needs further improvement in the future. Moreover, in this paper, only single fault-bearing vibration signals are used for model training, and no compound fault samples are created to simulate the actual situation, which is a challenge for applying the proposed model in practical engineering. It has also become a research direction for us in the future.

References

- [1] Shengnan Tang; Shouqi Yuan; Yong Zhu. “Convolutional Neural Network in Intelligent Fault Diagnosis Toward Rotatory Machinery”. In: *IEEE Journals Magazine — IEEE Xplore*. (May 2020b), pp. 86510–86519. DOI: 10.1109/ACCESS.2020.2992692.
- [2] H. Kim and I. Joe. “An XAI method for convolutional neural networks in self driving cars”. In: *PLOS ONE* 17.8 (2022), e0267282. DOI: 10.1371/journal.pone.0267282.
- [3] E. Brusa et al. “Explainable AI for Machine Fault diagnosis: Understanding features’ contribution in machine learning models for industrial condition monitoring”. In: *Applied Sciences* 13.4 (2023), p. 2038. DOI: 10.3390/app13042038.
- [4] *Fault Data Sets - Society For Machinery Failure Prevention Technology*. URL: <https://www.mfpt.org/fault-data-sets/>.
- [5] H. Purohit. *MIMII Dataset: Sound Dataset for Malfunctioning Industrial Machine Investigation and Inspection*. Zenodo. 2019. DOI: 10.5281/zenodo.3384388.
- [6] *Saintmartin Travels: Dhaka-Chittagong-Cox’s bazar-Teknaf*. URL: <https://saintmartintravels.com/>.
- [7] Z. Xie et al. “Ball screw fault diagnosis based on continuous wavelet transform and two-dimensional convolution neural network”. In: *Measurement & Control*(2022), p. 002029402211076. DOI: 10.1177/00202940221107620.
- [8] A. Choudhary, T. Mian, and S. S. Fatima. “Convolutional neural network- based bearing fault diagnosis of rotating machine using thermal images”. In: *Measurement* 176 (2021), p. 109196. DOI: 10.1016/j.measurement.2021.109196.

- [9] R. Liu et al. “Artificial intelligence for fault diagnosis of rotating machinery: A review”. In: *Mechanical Systems and Signal Processing* 108 (2018), pp. 33–47. DOI: 10.1016/j.ymssp.2018.02.016.
- [10] C. Chen et al. “An Improved Fault Diagnosis Using 1D-Convolutional Neural Network Model”. In: *Electronics* 10.1 (2020), p. 59. DOI: 10.3390/electronics10010059.
- [11] Q. Xu et al. “Fault diagnosis of rolling bearing based on online transfer convolutional neural network”. In: *Applied Acoustics* 192 (2022), p. 108703. DOI: 10.1016/j.apacoust.2022.108703.
- [12] R. Yan, R. X. Gao, and X. Chen. “Wavelets for fault diagnosis of rotary machines: A review with applications”. In: *Signal Processing* 96 (2014), pp. 1–15. DOI: 10.1016/j.sigpro.2013.04.015.
- [13] D. V. Hoang and H. Kang. “Rolling element bearing fault diagnosis using convolutional neural network and vibration image”. In: *Cognitive Systems Research* 53 (2019), pp. 42–50. DOI: 10.1016/j.cogsys.2018.03.002.
- [14] R. Zhao et al. “Deep learning and its applications to machine health monitoring”. In: *Mechanical Systems and Signal Processing* 115 (2019), pp. 213–237. DOI: 10.1016/j.ymssp.2018.05.050.
- [15] M. Fernandes, J. M. Corchado, and G. Marreiros. “Machine learning techniques applied to mechanical fault diagnosis and fault prognosis in the context of real industrial manufacturing use-cases: a systematic literature review”. In: *Applied Intelligence* 52.12 (2022), pp. 14246–14280. DOI: 10.1007/s10489-022-03344-3.


- [16] R. Liu et al. “Artificial intelligence for fault diagnosis of rotating machinery: A review”. In: *Mechanical Systems and Signal Processing* 108 (2018), pp. 33–47. DOI: 10.1016/j.ymssp.2018.02.016.
- [17] A. Choudhary, T. Mian, and S. S. Fatima. “Convolutional neural network based bearing fault diagnosis of rotating machine using thermal images”. In: *Measurement* 176 (2021), p. 109196. DOI: 10.1016/j.measurement.2021.109196.
- [18] G. S. Martin et al. “Deep variational auto-encoders: A promising tool for dimensionality reduction and ball bearing elements fault diagnosis”. In: *Structural Health Monitoring-an International Journal* 18.4 (2018), pp. 1092–1128. DOI: 10.1177/1475921718788299.
- [19] Z. Zhang et al. “General normalized sparse filtering: A novel unsupervised learning method for rotating machinery fault diagnosis”. In: *Mechanical Systems and Signal Processing* 124 (2019), pp. 596–612. DOI: 10.1016/j.ymssp.2019.02.006.
- [20] *A Novel Deeper One-Dimensional CNN With Residual Learning for Fault Diagnosis of Wheelset Bearings in High-Speed Trains*. URL: <https://ieeexplore.ieee.org/abstract/document/8584445>.
- [21] *Convolutional Neural Networks, Explained - Towards Data Science*. URL: <https://towardsdatascience.com/convolutional-neural-networks-explained-9cc5188c4939>.
- [22] *Different Types of CNN Architectures Explained: Examples - Data Analytics*. URL: <https://vitalflux.com/different-types-of-cnn-architectures-explained-examples/>.
- [23] J. Zhang et al. “Fault Diagnosis of Reciprocating Machinery based on improved MEEMD-SqueezeNet”. In: *Measurement* (2023), p. 113026. DOI: 10.1016/j.


measurement.2023.113026.

- [24] Y. Chandola et al. “End-to-end pre-trained CNN-based computer-aided classification system design for chest radiographs”. In: *Elsevier eBooks*. 2021, pp. 117–140. DOI: 10.1016/b978-0-323-90184-0.00011-4.
- [25] *Activation functions: ReLU vs. Leaky ReLU - MLearning.ai - Medium*. URL: <https://medium.com/mlearning-ai/activation-functions-relu-vs-leaky-relu-b8272dc0b1be>.
- [26] “An Intelligent Deep Feature Learning Method With Improved Activation Functions for Machine Fault Diagnosis”. In: *IEEE Journals & Magazine — IEEE Xplore* (2020). DOI: 10.1109/ACCESS.2019.2955751.
- [27] *Neural Network: The Dead Neuron - Towards Data Science*. URL: <https://towardsdatascience.com/neural-network-the-dead-neuron-eaa92e575748>.
- [28] *Deep convolutional and LSTM recurrent neural networks for rolling bearing fault diagnosis under strong noises and variable loads*. URL: <https://ieeexplore.ieee.org/document/9056473>.
- [29] H. Shao et al. “Rolling bearing fault detection using continuous deep belief network with locally linear embedding”. In: *Computers in Industry* 96 (2018), pp. 27–39. DOI: 10.1016/j.compind.2018.01.005.
- [30] X. Li et al. “Rolling bearing health prognosis using a modified health index based hierarchical gated recurrent unit network”. In: *Mechanism and Machine Theory* 133 (2019), pp. 229–249. DOI: 10.1016/j.mechmachtheory.2018.11.005.

- [31] D. Hoang and H. Kang. “Rolling element bearing fault diagnosis using convolutional neural network and vibration image”. In: *Cognitive Systems Research* 53 (2019), pp. 42–50. DOI: 10.1016/j.cogsys.2018.03.002.
- [32] K. Lakhdari and N. Saeed. “A new vision of a simple 1D Convolutional Neural Networks (1D-CNN) with Leaky-ReLU function for ECG abnormalities classification”. In: *Intelligence-based Medicine* 6 (2022), p. 100080. DOI: 10.1016/j.ibmed.2022.100080.
- [33] A. Mujhid et al. “Comparison and combination of leaky RELU and RELU activation function and three optimizers on Deep CNN for COVID-19 detection”. In: *Frontiers in artificial intelligence and applications* (2022). DOI: 10.3233/faia220369.
- [34] *Rolling Element Bearing Fault Diagnosis Using Deep Learning - MATLAB & Simulink*. URL: <https://www.mathworks.com/help/predmaint/ug/rolling-element-bearing-fault-diagnosis-using-deep-learning.html>.
- [35] *Deep Residual Learning for Image Recognition*. URL: <https://ieeexplore.ieee.org/document/7780459>.
- [36] *Confusion Matrix in Machine Learning - Javatpoint*. URL: <https://www.javatpoint.com/confusion-matrix-in-machine-learning>
- [37] Aliano, S. (2023, August 25). World’s Largest Manufacturers Lose \$1 Trillion/Year to Machine Failure. World’s Largest Manufacturers Lose \$1 Trillion/Year to Machine Failure. <https://blog.isa.org/worlds-largest-manufacturers-lose-1-trillion/year-to-machine-failure>

Appendix A.

run by  HYUNDAI UNIVERSE



Saintmartin Travels Ltd.

Committed to your pleasure tour

24th June 2023

To Whom It May Concern,

This letter serves to authorize **Sanjana Khan Shammi**, a student of **BRAC University**, to conduct data collection for her thesis on machine fault diagnosis from our company **Saintmartin Travels**.


We understand and support the importance of research in the field of engineering and technology. As such, we have no objections in permitting **Sanjana Khan Shammi** to collect data from our premises for her research. She will be given full access to our machines and equipment for data collection purposes only.

We hereby grant **Sanjana Khan Shammi** permission to collect data regarding machine fault diagnosis. She will be required to follow all the safety protocols and regulations set forth by our company while on site.

We trust that **Sanjana Khan Shammi** will conduct her research responsibly, and we wish her the best of luck for their thesis.

Sincerely,

Saintmartin Travels Ltd.



Director

Office: 167/2 Eaden Complex, Arambag, Motijheel, Dhaka-1000. Cell: 01972 843355